

## Roll-to-Roll Fabrication of Solution Processed Electronics

Abbel, Robert; Galagan, Yulia; Groen, Pim

**DOI**

[10.1002/adem.201701190](https://doi.org/10.1002/adem.201701190)

**Publication date**

2018

**Document Version**

Final published version

**Published in**

Advanced Engineering Materials

**Citation (APA)**

Abbel, R., Galagan, Y., & Groen, P. (2018). Roll-to-Roll Fabrication of Solution Processed Electronics. *Advanced Engineering Materials*, 20(8), 1-30. Article 1701190. <https://doi.org/10.1002/adem.201701190>

**Important note**

To cite this publication, please use the final published version (if applicable).  
Please check the document version above.

**Copyright**

Other than for strictly personal use, it is not permitted to download, forward or distribute the text or part of it, without the consent of the author(s) and/or copyright holder(s), unless the work is under an open content license such as Creative Commons.

**Takedown policy**

Please contact us and provide details if you believe this document breaches copyrights.  
We will remove access to the work immediately and investigate your claim.

***Green Open Access added to TU Delft Institutional Repository***

***'You share, we take care!' - Taverne project***

**<https://www.openaccess.nl/en/you-share-we-take-care>**

Otherwise as indicated in the copyright section: the publisher is the copyright holder of this work and the author uses the Dutch legislation to make this work public.



Pushing the boundaries  
of chemistry?  
It takes  
#HumanChemistry

Make your curiosity and talent as a chemist matter to the world with a specialty chemicals leader. Together, we combine cutting-edge science with engineering expertise to create solutions that answer real-world problems. Find out how our approach to technology creates more opportunities for growth, and see what chemistry can do for you at:

[evonik.com/career](https://evonik.com/career)



# Roll-to-Roll Fabrication of Solution Processed Electronics

Robert Abbel, Yulia Galagan, and Pim Groen\*

The production of electronic devices using solution based (“wet”) deposition technologies has some decisive technical and commercial advantages compared to competing approaches like vacuum based (“dry”) manufacturing. Particularly, the potential to scale up production processes to large areas and high volumes by introducing continuous roll-to-roll (R2R) methods on flexible substrates has been the topic of intense studies from both applied research institutes and industry already for some years. Decisive steps forward have been achieved during that time, resulting in the dawn of commercial applications for a number of processes, while additional development work is still needed in some other fields. This review summarizes the work published during the last few years on the R2R printing and wet coating of electronic devices. An overview is presented of the basic operational principles for the most commonly used R2R printing and coating methods and techniques for proper web handling in R2R lines. Then, the most commonly used types of flexible substrate materials are introduced, followed by a review of the work published in the application areas of transparent conductor materials, printed electric connections, light emitting devices, photovoltaic energy generation, printed logic, and sensing.

sheet-to-sheet (S2S) processing is based on its capabilities for high throughput and large area mass manufacturing, which allow to increase product output and reduce production costs.<sup>[2,4,5]</sup> With respect to electronics and optoelectronics devices, R2R processing is for many applications still in the research and development phase, although commercial manufacturing is starting to be implemented for a number of relatively simple product types like smart cards.<sup>[2]</sup> For more complicated appliances like solar cells, transistors and light emitting devices, R2R printing and coating are in addition competing with vacuum based S2S and R2R deposition methods like evaporation and sputtering which achieve patterning by masking and photolithographic techniques.<sup>[6–8]</sup> Whereas the latter typically offer higher product quality in terms of pattern resolution and definition, registration accuracy, device performance, and product lifetime, the need for vacuum based processing complicates manufacturing processes and strongly increases production costs.<sup>[9]</sup> The

## 1. Introduction

Roll-to-roll (R2R) processing by wet deposition methods using solutions and dispersions of functional materials (i.e., inks and pastes) is a mature and extensively used manufacturing method in the printing and coating industries. It is employed for a wide variety of applications, ranging from packaging and paper production to functional membranes, photographic films, thin film batteries, and textiles.<sup>[1–3]</sup> Its particular attractiveness for industrial production compared to the alternative approach of


potential of R2R printed and coated electronics products is, therefore, generally seen in the market for ubiquitous low-cost, low-end, and potentially single-use disposable devices rather than in the high-end customer electronics sector.<sup>[10,11]</sup> Possible application areas are smart packaging with integrated sensors and signage components, smart cards, wearable electronics, for example, health care monitoring, or energy harvesting devices like solar cells integrated in clothing and other articles.<sup>[12,13]</sup> For many of these application fields, the mechanical flexibility and integrity of the electronic components is a particularly beneficial design feature.<sup>[13,14]</sup> In contrast to S2S processing, which is typically done on rigid carriers, for obvious reasons R2R manufacturing intrinsically requires its substrates and products to be bendable at least to some degree.

This review provides an overview about the current state of the scientific literature regarding the R2R processing of various electronic and optoelectronic devices by wet deposition technologies, that is, printing and coating. S2S manufacturing and “dry”, that is, vacuum-based approaches have not been included. For more information on these topics, the reader is referred to a number of already published books and reviews.<sup>[6,15,16]</sup> The review will start with a short introduction of R2R printing, coating, and web handling technologies, and then proceed with a discussion of the most commonly used substrate materials and their properties. Subsequently, several sections will follow on R2R wet processing of (opto)electronic

Prof. Dr. P. Groen, Dr. R. Abbel, Dr. Y. Galagan  
Holst Centre – TNO  
High Tech Campus 31  
Eindhoven, 5656 AE, The Netherlands  
E-mail: pim.groen@tno.nl

Prof. Dr. P. Groen  
Faculty of Aerospace Engineering  
Delft University of Technology  
Kluyverweg 1, Delft, 2629 HS Delft, The Netherlands

Dr. Y. Galagan  
Holst Centre – Solliance  
High Tech Campus 21  
Eindhoven, 5656 AE, The Netherlands

 The ORCID identification number(s) for the author(s) of this article can be found under <https://doi.org/10.1002/adem.201701190>.

DOI: 10.1002/adem.201701190

materials and devices for the application areas of transparent conductors, printed circuitry and electric connections, light emitting devices, photovoltaic cells, transistors and logic, sensors, and newly emerging applications. A summary and conclusions part will finish the review.

## 2. R2R Printing/Coating Techniques

A wide variety of printing and coating techniques have been applied to R2R printed electronics, some of which are by themselves particularly suited for R2R processing due to their intrinsic mode of operation, whereas others need to be specifically adjusted to be R2R compatible.<sup>[17]</sup> Many reviews and textbooks describing the technologies in detail are available in the open literature,<sup>[1,18–24]</sup> which is why we constrain ourselves here to a brief introduction.

Generally, printing technologies can be divided into two classes, depending on whether the ink transfer onto the substrate occurs with or without direct physical contact of the printing equipment with the surface to be printed on. Contact printing methods are thus distinguished from non-contact printing technologies. A schematic overview of R2R printing technologies is provided in **Figure 1**. Whereas in the case of contact printing techniques, the ink is deposited using a stamp or mold, which potentially can damage pressure sensitive underlying functional layers, this disadvantage is avoided for the non-contact approach, where ink droplets are produced close to the substrate, but at some distance, and then are propelled across the gap. This is particularly useful when mechanically sensitive substrates are used, which can easily be damaged by physical contact, like moisture and oxygen barrier coatings on polymer films.<sup>[25–27]</sup> The only non-contact printing technique which has been widely employed so far for the R2R production of functional electronic materials is inkjet printing (IJP).<sup>[22,28]</sup> Here, low viscosity inks are ejected in the form of droplets by a pressure pulse in a nozzle, which is either created by heat-induced partial evaporation of the ink (thermal IJP) or by an electric voltage pulse applied to a piezo element (piezoelectric IJP). IJP is very flexible from a design point of view, because the desired pattern can be adjusted simply by changes to the digital design definition file and no hardware adjustments are necessary. In R2R applications, the limiting factor for processing speed are the frequency and reliability of droplet formation and position control, which is why it is typically not faster than a few  $\text{m min}^{-1}$ .<sup>[20,28]</sup> Achievable layer thicknesses are usually quite low (a few hundreds of nm at most) and for high-throughput production, the reliable feature resolution is limited to about 15–20  $\mu\text{m}$ .<sup>[20,28]</sup> Structures in the submicron range have, however, been reported using special techniques like electrostatic IJP, which have not yet been applied to R2R processing, though.<sup>[29]</sup>

All contact printing technologies make use of some pre-defined stencil or mold, which defines the pattern to be deposited. In the case of offset, gravure, and flexo printing, these pre-defined patterns are imprinted on rolls which ultimately transfer the inks from a reservoir onto the substrate.<sup>[1,18]</sup> Therefore, changes in the printed pattern require a redesign of the printing rolls, rendering this family of techniques less



Robert Abbel received his PhD degree from Eindhoven University of Technology (The Netherlands) on the supramolecular chemistry of  $\pi$ -conjugated oligomers. In 2009, he joined Holst Centre's technology program "Printed Conductive Structures", where he was responsible for materials and process development for the Printed Electronics industry. Since 2015, he is Senior Scientist in Holst Centre's research groups on "Large Area Coating" and "Printed Organic Lighting and Signage".



Yulia Galagan is a Senior Scientist at Holst Centre and Solliance. She received her PhD in chemistry in 2002 from Kyiv University. She was a post-doctoral researcher at National Taiwan University, and in 2008 she joined Holst Centre. Her research interests are focused on organic and perovskite-based electronics and on emerging photovoltaic technologies.

Currently Yulia Galagan is responsible for technology development for roll-to-roll manufacturing of perovskite photovoltaics.



Pim Groen is working at Holst Centre – TNO as program manager "Large Area Coating" and has earlier also led the research program on "Printed Conductive Structures". In addition, since 2012 he is part time professor on Smart Materials at Delft University of Technology. He studied chemistry at Leiden University and did his PhD on ceramic cuprate superconductors. Hereafter he worked for Philips Research on inorganic materials and ceramics for lighting and passive component applications.

particularly suited for R2R applications and can provide very high web handling speeds of up to several hundred  $\text{m min}^{-1}$  in established industrial manufacturing processes.<sup>[1]</sup>

A completely different approach of contact printing is screen printing, where the ink is squeezed through a fine mesh of threads or wires, and the openings between them are locally blocked in order to define the printing pattern. It can be applied to R2R processing in the form of rotary screen printing, where the ink transfer occurs from the interior of a roll into which the screen has been bent, but also flatbed screen printing is possible on flexible substrates transported on rolls.<sup>[1]</sup> Screen printing is particularly suited for paste-like functional inks with high viscosities and typically deposits structures with heights of several tens to a few hundred micrometers and a pattern



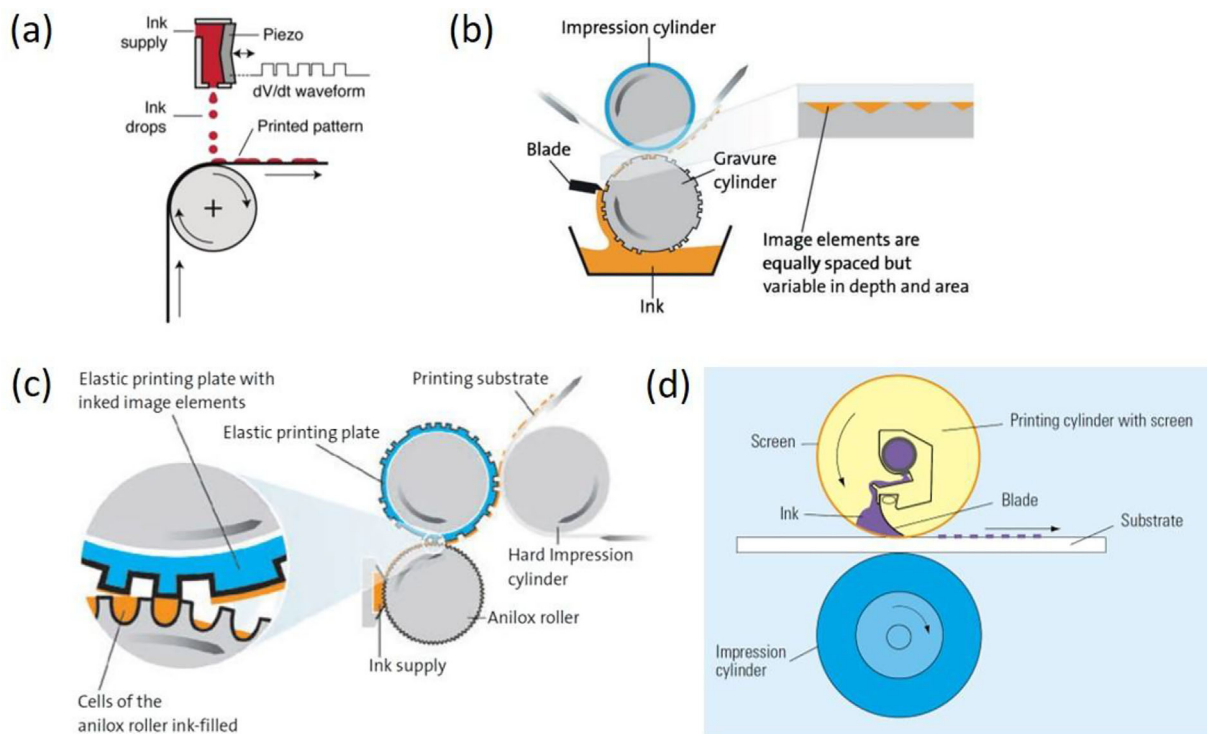


**Figure 1.** Schematic overview of some commonly used R2R printing technologies for electronics manufacturing. a) Inkjet printing. Reproduced with permission from ref. [32]. Copyright 2013 Wiley. b) Gravure printing. Reproduced with permission from ref. [33]. Copyright 2017 Organic and Printed Electronics Association. c) Flexo printing. Reproduced with permission from ref. [33]. Copyright 2017 Organic and Printed Electronics Association. d) Rotary screen printing. Reproduced with permission from ref. [1]. Copyright 2011 Springer Verlag.

resolution comparable to that of IJP. As in the case of offset, gravure and flexo printing, design changes require hardware adaptations, in this case in the form of a dedicated new screen. For printed electronics applications, production speeds of  $10 \text{ m min}^{-1}$  and above have been demonstrated, making the technology well suited for industrial applications.<sup>[20,31]</sup>

Coating differs from printing in its potential to produce uniform and homogeneous functional films over large areas, whereas the strength of printing technologies is the possibility to deposit well-defined patterned structures with high resolution. Although some limited degree of patterning can also be achieved by specialized coating methods like stripe and intermittent coating, both the degree of design freedom and the resolution of the resulting structures are much higher for printing techniques. In principle, all printing technologies can of course also be employed for full area deposition by refraining from using any pattern input, but dedicated coating techniques are usually preferred because they offer better control over film thickness homogeneity and surface roughness.<sup>[23]</sup> A schematic overview about various R2R coating technologies is provided in **Figure 2**. In contrast to most printing techniques, coating is also usually done in a non-contact mode, which can constitute an additional advantage if mechanically sensitive substrates are used. A straightforward and frequently applied method to deposit rather thick functional films (a few hundreds of nm to several tens of  $\mu\text{m}$ ) is blade (or knife) coating, where the deposited film thickness is mainly determined by the distance of the coating

blade from the substrate, which is moving underneath.<sup>[34,35]</sup> Somewhat more sophisticated is slot die coating, where the ink is squeezed through a very well-defined slit and the film thickness is controlled by the ink flow rate and the web speed.<sup>[36]</sup> In contrast to blade coating, slot die coating has some potential for patterning, albeit limited to stripes and rectangles. In order to achieve this, the ink flow is either limited spatially in the direction of the web movement by the use of inserts (shims) or specially designed slot die slits (stripe coating<sup>[37,38]</sup>), or it is interrupted by controlled starting and stopping, resulting in patterning orthogonal to the coating direction (intermittent coating<sup>[38–40]</sup>). A completely different approach is spray coating, where an aerosol of fine ink droplets is created and deposited homogeneously on the substrate.<sup>[41]</sup> Its application in R2R lines is quite straightforward and it has been used, for example, for the deposition of electrodes for supercapacitors.<sup>[42]</sup>

### 3. R2R Web Handling

Another important aspect of R2R coating and printing is control over the substrate handling in the processing line at a specified speed, tension and alignment perpendicular to the web movement. Whereas from a mass production point of view, high processing speeds are desired, for obvious reasons control over resolution and registration accuracy tends to get more challenging with increasing web velocities.<sup>[43,44]</sup> Also, post-

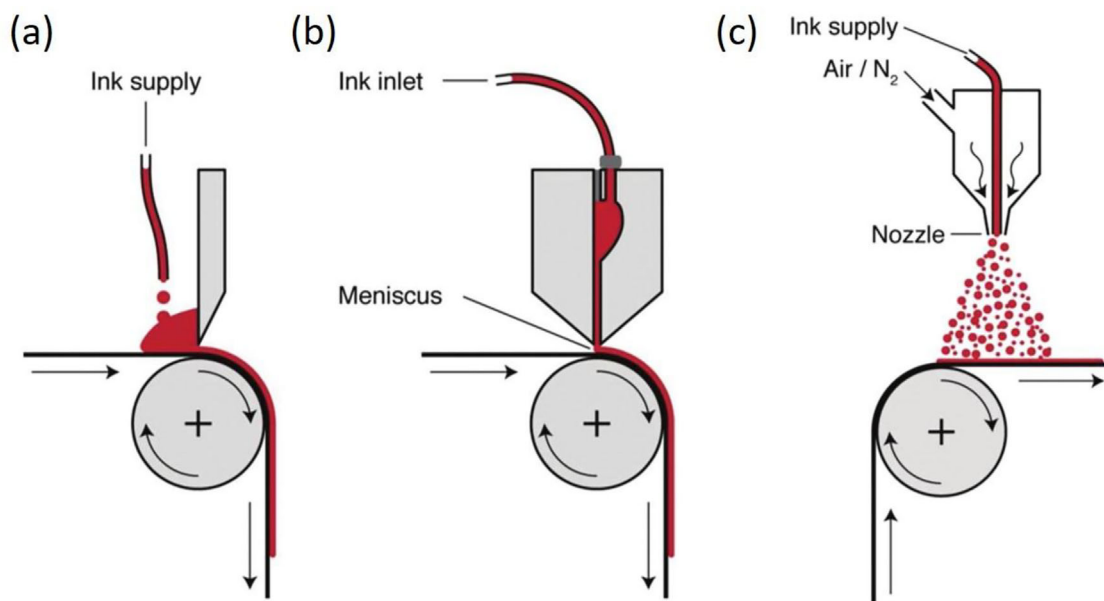


**Figure 2.** Schematic overview of some commonly used R2R coating technologies for electronics manufacturing. a) Blade coating, b) slot die coating, c) spray coating. All images reproduced with permission from ref. [32]. Copyright 2013 Wiley.

treatment steps like drying and annealing can take significant time and thus put their own restrictions on the processing speeds. In the field of R2R printed electronics, good registration accuracy is crucial for device quality and yield, because frequently, several layers need to be deposited on top of each other with high positional precision, sometimes even using different printing technologies.<sup>[45]</sup> This is of particular importance for all research areas where device architectures are constantly proceeding toward smaller dimensions, like thin film transistors (TFTs; **Figure 3**,<sup>[43,46]</sup>). Another reason for precise control over the web movement is that coating thicknesses often depend on the substrate speed and can be correctly achieved only if the process has actually been operated exactly at the predetermined velocity. This has been demonstrated by Park et al., who R2R slot die coated an antireflective layer on a poly(ethylene terephthalate) (PET) substrate at  $1.6\text{--}4.4\text{ m min}^{-1}$  in order to improve organic photovoltaic (OPV) efficiencies.<sup>[47]</sup> Both by modeling and by experiment, they showed that in addition to the solid contents of the coating ink, the web speed is a crucial parameter to control film thickness. In-line process monitoring of the structure definition during R2R production is thus crucial to achieve high product yields. One example is the thickness measurement setup for printed conductive structures based on capacitive and eddy current sensors which Seong et al. have developed and installed on a R2R printing line.<sup>[48]</sup> Another one is the monitoring by in-line X-ray scattering of the drying behavior of OPV polymers, which have been R2R slot die coated on PET films.<sup>[49]</sup>

The web tension must be precisely controlled in order to prevent substrate deformation, particularly at elevated temperatures, which is another possible source for decreased overlay accuracy or damage to functional layers (**Figure 3**<sup>[46,50,51]</sup>). It has been shown that the web tension can even have an influence on

the definition of single layer structures.<sup>[52]</sup> One possible mechanism was identified by Lee et al., who showed that stress variations from handling in a R2R line can alter the surface properties of the substrate. This can result in inconsistent quality of the functional structures printed on them, even when all other processing parameters are kept unchanged.<sup>[53]</sup> Uncontrolled web tension variations during operation can also directly damage the printed structures and decrease their performance, especially if they occur at high temperatures, where many plastic films are more prone to elongation under stress. This has been demonstrated by Kang and Lee, using the example of R2R gravure printed silver lines which were dried at  $150\text{ }^{\circ}\text{C}$  and cracked when put under tension, resulting in a tenfold decrease of their electrical conductivity at 60% strain, but even much smaller elongations (10% and below) already caused significant damage (**Figure 3**<sup>[54]</sup>). Web tension in a R2R line can be controlled either by direct feedback using load cells, or indirectly by using linear or pendulum dancers.<sup>[50,55,56]</sup> In order to provide fast and precise correction input to quickly restore the desired web tension and velocity once a deviation from the specified values has been detected, suitable algorithms have been developed and experimentally tested.<sup>[57]</sup> An additional complication is, however, that web tension corrections carried out by web speed variations sometimes tend to introduce registration errors in themselves.<sup>[58]</sup> For position control of the web and thus high registration accuracy of fine patterns (both laterally and in the web transport direction), optical control systems are frequently employed which detect registration marks printed next to the actual functional structures.<sup>[59]</sup> Experimental testing has shown overlay accuracies down to  $2.5\text{ }\mu\text{m}$  at web speeds of  $2\text{ m min}^{-1}$  to be possible.<sup>[59]</sup> Also in this case, efficient algorithms were needed to provide the required feedback as quickly as possible to correct misalignment on the fly.<sup>[60]</sup> Using a

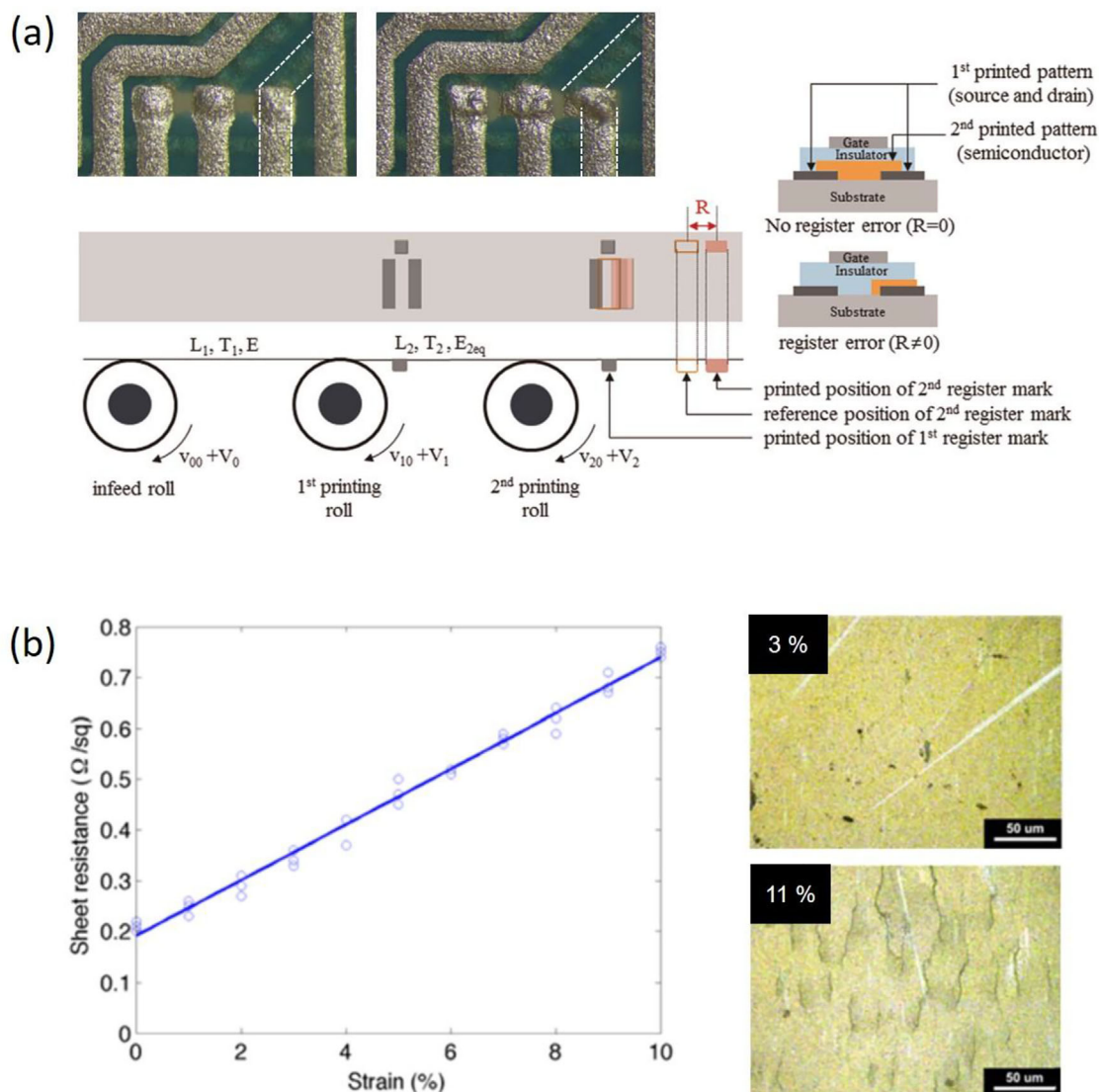


**Figure 3.** Negative effects of uncontrolled web handling. a) Misalignment (registration errors) of printed functional layers in TFT devices. Reproduced with permission from ref. [46]. Copyright 2015 Elsevier. The inset image shows multilayer prints (silver/isolator/silver) with well aligned (left) and misaligned (right) metal structures. Courtesy of Milan Saalmink, Holst Centre. b) Damage to printed structures due to improper web handling: sheet resistance of R2R gravure printed silver structures as a function of film strain and optical micrographs of samples subjected to various amounts of strain. Adapted from ref. [54] with permission. Copyright 2015 Springer Verlag.

R2R printing line with such control equipment, Kim et al. were able to demonstrate well-controlled multilayer printing of conductive patterns by the gravure-offset, gravure, and flexo techniques.<sup>[61]</sup>

#### 4. Substrates

For R2R processing to be applicable, the used substrates obviously need to display a certain degree of mechanical flexibility. Several types of substrate materials have been reported for use in R2R manufacturing, the most important ones being

thin glass,<sup>[62,63]</sup> polymer films,<sup>[20,64]</sup> and metal foils or metallized polymer films.<sup>[65–67]</sup> For certain applications, also paper substrates have been used.<sup>[68]</sup> All have their distinct advantages and disadvantages with respect to each other. Both glass and polymer films are optically transparent, with glasses typically having the wider optical window, particularly into the near-UV region.<sup>[62]</sup> For optoelectronic applications which depend on the interaction with light, this enables the built-up of structures where the light enters or leaves the devices through the substrate. In the case of light emitting devices (OLEDs and LECs), this design is known as bottom-emissive.<sup>[69]</sup> On non-transparent metal foils (and also paper, where applicable), for



obvious reasons, any interaction with light needs to occur away from the substrate surface, resulting in top-emissive devices as the only option in this case.

Many materials used in organic optoelectronic devices are highly sensitive to degradation by reaction with water or oxygen from the ambient environment. This particularly applies to the electronically active layers in OLEDs and photovoltaic devices. As a consequence, these layers typically not only need to be processed under the exclusion of air and moisture, but also must be effectively sealed from the environment. This can be achieved by encapsulation techniques which suppress the diffusion of degrading agents into the active layers or at least slow it down to such a degree that no significant performance decrease occurs during product lifetime. Whereas thin glass has excellent intrinsic barrier properties, hardly deforms under stress and expands only slightly at elevated temperatures, it is susceptible to breaking when being bent too strongly.<sup>[62]</sup> While this risk can be mitigated by laminating the glass on a polymer carrier prior to the coating step, this approach puts a certain limit on the maximum processing temperatures, as the thermal stability of the carrier film will be significantly lower than that of the bare glass. Also, breaking glass releases chips that are difficult to remove from the coating line or drying ovens and can cause serious particle contamination. Thinner glass is preferred in this respect to thicker glass, as the stresses building up during bending increase with substrate thickness. The peculiarities in handling thin glass in a R2R setup compared to non-breakable substrates are described by Deus et al.<sup>[63]</sup> Metal foils display barrier properties comparable to those of thin glass and are also very stable against stretching under stress, but require very careful web handling, as they tend to wrinkle irreparably, which can lead to serious problems for device performance. Due to their porosity, paper substrates are not suited for printed electronic applications which require the strict exclusion of moisture or oxygen but can be employed when only environmentally stable materials are used, for example, in the case of smart cards. The most commonly used substrate materials are polymer films, which are available at low cost, do not splinter and, in contrast to metal foils and thin glass, are relatively forgiving with regards to deformation from improper web handling. On the other hand, they do not exhibit sufficient water and oxygen barrier properties for many electronic applications and thus must be endowed with an additional barrier coating.<sup>[26]</sup> Furthermore, their maximum processing temperatures are limited by their glass transition point, which, depending on the exact material, can be anywhere between 80 °C and several hundreds of °C.<sup>[64,70]</sup> The latter materials with high thermal stability (e.g., polyimide), however, tend to be quite costly and are only applied when no cheaper alternatives are available. Even at temperatures far below their glass transition, most polymer substrates tend to stretch under the significant stresses which are often applied during R2R processing, because their Young's moduli are much lower than those of glass or metals. This deformation during web handling is important to understand, quantify and control, as it poses limits on registration accuracy when several functional layers with high resolution patterning need to be deposited on top of each other with high precision.<sup>[46]</sup> Lee and Yoo have dedicated an in-depth study on the mechanical behavior of relevant plastic substrates under stress from R2R

gravure printing and found that heat stabilized PET displayed a higher mechanical and thermal stability than biaxially oriented polypropylene.<sup>[70]</sup> A similar study by MacDonald et al., which included also characteristics like stability against common solvents, water uptake and surface quality, has demonstrated that poly(ethylene naphthalate) (PEN) is, from a technical point of view, generally better suited than PET for higher demanding processing conditions, which can justify its use, despite its higher price.<sup>[64]</sup>

In addition to serving merely as carriers, certain substrates also fulfil specific functions critical for device operation. In the rather obvious case of metal foils, their intrinsic excellent electric conductivity is typically used to connect the finished devices to the power supply system. Frequently, however, some type of structuring, for example, by the deposition of an isolating material, is needed to produce functional devices. In the case of optoelectronic devices such as bottom emissive OLEDs or solar cells, transparent substrates, such as polymer films and thin glass, also interact with the generated or incident light by internal reflection and scattering. For non-optimized device structures, this can result in significant light losses and strongly reduced efficiencies.<sup>[71]</sup> A proper choice of the substrates' thicknesses, refractive indices and internal and surface structures can be employed to improve device performances, for example, by an enhanced degree of light in- or outcoupling, respectively. Sato et al. have demonstrated the R2R production of substrates with corrugated surface structures using nano-imprinting of structures formed originally by block-copolymer self-assembly.<sup>[72]</sup> Polymer light emitting electrochemical cells (LECs) produced on these corrugated substrates were up to two times more efficient than reference devices made on flat substrates, without compromising the spectral properties or angular characteristics of the emitted light. This improvement was attributed to an enhanced outcoupling of the generated light.

Surface roughness is another critical substrate property which influences the performance and yield of devices deposited on top of them. As in most cases, the functional layers applied are very thin (in the order of several nanometers to a few micrometers), their uniformity is easily disturbed by surface defects. Notwithstanding the necessity for surface structuring in certain cases, for example, on metal foils as described above, typically substrates are preferred which are as flat as possible. Therefore, the use of paper substrates is prohibitive for a number of applications, whereas others are more forgiving, particularly when relatively thick layers are employed. With respect to surface roughness, thin glass tends to perform better than polymer films or metal foils, with  $R_a$  values significantly below 0.5 nm, as opposed to several nanometers for both alternatives.<sup>[62]</sup> On the latter substrates, some kind of planarization layer frequently needs to be applied to allow proper device performance.

## 5. Printing and Coating of Transparent Conductors

The functionality of any optoelectronic device, for example, an OLED or a solar cell, is defined by the interaction and interconversion of electric energy and light. As a consequence

of their typical architecture which consists of a complex stack of thin functional layers, there is a need for at least one electrode to be at the same time electrically conductive and transparent to visible light. In order to characterize the capacity of a thin film to transport electrical current in the lateral (in-plane) direction, the sheet resistance is most commonly reported, which, in contrast to the volume resistivity, is inversely proportional to the film thickness. While a thicker conductive film thus results in a lower sheet resistance, at the same time its light transmission will decrease, which requires a balance to be determined for ideal device performance, depending on the exact requirements of the application. To further improve the sheet resistance of the transparent conductor, especially over large areas, an additional printed grid can be used, as is explained in the next section. By far the most commonly used materials for transparent electrodes are indium tin oxide (ITO) and fluorine doped tin oxide (FTO), which have some undisputed merits in terms of transparency and sheet resistance ( $T > 90\%$  and  $R_{sq} < 10 \Omega \text{sq}^{-1}$ ).<sup>[73]</sup> However, for high quality films they need to be deposited by vacuum based dry technologies (sputtering). In addition, optimum performance is only achieved after annealing at temperatures which most flexible polymer substrates cannot withstand. Furthermore, transparent conductive oxides are mechanically brittle which limits device flexibility, and ITO is based on scarce and relatively expensive minerals.<sup>[74]</sup> Therefore, a number of alternative materials have been developed in order to replace indium for use in transparent conductors, some of which have also been deposited from solution or dispersion by R2R technologies.<sup>[74]</sup> The most important ones are treated individually in this section.

Conductive polymers are organic macromolecules based on conjugated monomers, which exhibit some (usually limited) degree of electrical conductivity, typically resulting, at film thicknesses which correspond to acceptable transparencies, in rather high sheet resistances. As a consequence, current transport in the lateral direction proceeds only over short distances, and for application in large area devices, conductive polymer films need to be supported by highly conductive grid structures. A blend of poly(ethylene dioxythiophene) and poly(styrene sulfonic acid) (PEDOT:PSS) is the most popular conductive polymeric material and can also serve as hole injection material in OLEDs or hole extraction material in solar cells. Roll-to-sheet gravure printing of PEDOT:PSS on PET at rather high speed ( $36 \text{ m min}^{-1}$ ) has been demonstrated by Sico et al., who have achieved  $130 \Omega \text{sq}^{-1}$  at more than 80% transmission (at 550 nm).<sup>[75]</sup> Thicker layers were obtained by multiple printing, which also had a positive effect on the surface roughness. The suitability of the transparent conductor films thus prepared was demonstrated by their application in S2S deposited OPV devices. In a later paper by Montanino et al. from the same research group, the addition of 5 vol% DMSO to the ink formulation gave an improved performance of  $125 \Omega \text{sq}^{-1}$  at a transmission of 90% at 550 nm at a speed of  $60 \text{ m min}^{-1}$ .<sup>[76]</sup> In this case, the films were further processed by S2S techniques into functioning OLEDs. Hwang et al. have developed a R2R microgravure coating system, which they have used to deposit PEDOT:PSS on PET at  $0.3 \text{ m min}^{-1}$ .<sup>[77]</sup> However, the films suffered from a high surface roughness and no results on sheet resistance or transparency were reported. Also, many other

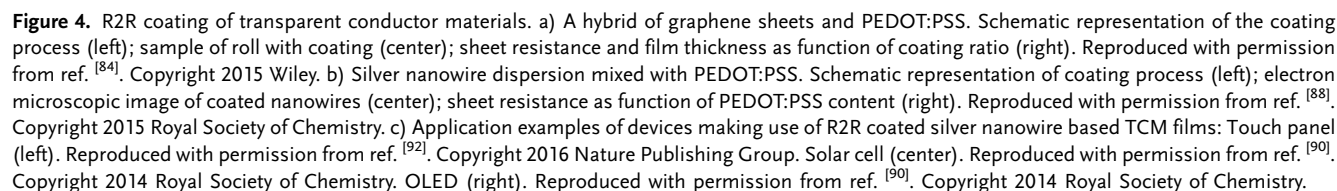
research groups have reported the coating of conducting polymers, particularly PEDOT:PSS, by R2R techniques, but in these cases, more functional layers for specific applications (PV, OLED etc.) were subsequently deposited, and these papers are summarized later in this review in the respective sections for the various device applications.

More recently, nanostructures based exclusively on carbon have proven their merits as transparent conductive electrodes as well. A particularly interesting material in this respect is graphene, which intrinsically displays a highly beneficial combination of sheet resistance and optical transmission; performance figures rivaling those of ITO have been reported, while the mechanical flexibility is much better.<sup>[78–81]</sup> Two main routes toward large area graphene coatings have been exploited, one being dry chemical vapor deposition (CVD), the other one the wet coating of dispersions of exfoliated graphene (or graphene oxide) platelets.<sup>[81]</sup> Graphene oxide is more easily formulated into stable inks because it has a lower tendency toward agglomeration, but the resulting coatings need to be reduced in a separate step after deposition to restore the desired electrical properties of graphene. As a consequence of the two different preparation pathways, the dry and wet approaches result in very different microstructures, with CVD graphene generally exhibiting a much higher quality with large grain sizes and a low density of defects.<sup>[81]</sup> By contrast, solution processed graphene coatings are composed of small individual platelets, frequently even interdispersed with residual non-conductive ink additives, which can strongly impede charge transport. Therefore, their performance as transparent electrode materials is usually poorer than that of CVD graphene coatings. Nevertheless, there are many examples of devices containing S2S solution processed graphene as the transparent electrode. For those, the reader is referred to a number of review articles and the literature cited therein.<sup>[78–81]</sup> Demonstrations of graphene based transparent electrodes prepared by R2R solution based techniques are, by contrast, rather scarce.

An example which involves a R2R printing step of a graphene based ink has been published by Jang et al., but the entire process is rather complicated and contains many steps which are not easily scaled up to a continuous manufacturing mode.<sup>[82]</sup> A dispersion of reduced graphene oxide sheets was drop cast on silicone rubber stamps, which were then mounted on a roller and transferred onto a PET film via a dry R2R process at a rate of  $5 \text{ m min}^{-1}$ . After extended annealing (12 h at  $150^\circ \text{C}$ ), transparencies of 40–52% at 550 nm could be achieved; no absolute sheet resistance values were reported, though. On rigid glass substrates, however, sheet resistances of  $220 \text{ k}\Omega \text{sq}^{-1}$  were obtained by prolonged annealing. The conditions needed for this improvement, however (12 h at  $260^\circ \text{C}$ ), are not compatible with the PET substrates used for the R2R coating tests. The authors have prepared a flexible partially transparent capacitive touch sensor using their graphene coated PET films.

A more viable approach for fully continuous R2R manufacturing of graphene based inks is the one of Ning et al., who have reported the R2R rod coating of dispersed non-conductive graphene oxide sheets at  $0.5 \text{ m min}^{-1}$ .<sup>[83]</sup> Upon subsequent reduction by spray coating with a tin dichloride solution, these films could be partially reduced back to conductive graphene layers. After rinsing with ethanol to remove the reducer residues,

Recently, metal (mostly silver) nanowire networks, the most recent addition to the family of solution coatable TCMs, have attracted the most interest from the R2R coating community. This might be attributable to the fact that these materials tend to give significantly better TCM performances than can typically be achieved with conductive polymer, graphene, or nanotube



coatings, rivaling ITO on polymer substrates. R2R gravure printing of silver nanowire dispersions has been employed by a number of groups to produce conductive transparent films with reasonable ( $75 \Omega \text{ sq}^{-1}$  at more than 90% transmission) to excellent ( $5 \Omega \text{ sq}^{-1}$  at 92% transmission) properties, at coating speeds ranging from extremely slow ( $0.02 \text{ m min}^{-1}$ ) to rather fast ( $10 \text{ m min}^{-1}$ ; Figure 4).<sup>[87,88]</sup> In some cases, PEDOT:PSS was mixed with the nanowires to further improve the sheet resistance. In addition to simple drying, a number of studies employed more elaborate post-deposition techniques like laser welding<sup>[89]</sup> or exposure to solvents and compression rolling<sup>[90]</sup> in order to improve the sheet resistance even further. Top layers which prevent the nanowire coatings from degradation<sup>[91,92]</sup> or improve the electrical contact between the wires<sup>[93]</sup> have also been sometimes applied. Patterning has been achieved by locally selective photonic flash sintering through a mask and subsequent removal of uncured material.<sup>[94]</sup> In one case, the coated nanowire film has been embedded into a resin matrix and was then exposed by delamination from the original resin support, in order to achieve a particularly flat conductive surface.<sup>[95]</sup> Many application examples for the R2R coated conductive substrates have used pieces cut from the roll and produced a variety of devices by S2S technologies, ranging from transparent heaters<sup>[94]</sup> via printed touch panels<sup>[92]</sup> to organic solar cells<sup>[90]</sup> and lighting devices,<sup>[87,90,93,95]</sup> and OFETs.<sup>[90]</sup> An overview of the work done on R2R coated silver nanowire films is provided in Table 1 and some technology demonstrator devices are displayed in Figure 4.

## 6. Printed Circuitry and Electric Connections

Any electronic device needs some kind of highly conductive electric wiring or connections, either in order to be provided with electricity, or for the electric energy generated inside it to be extracted. The same is true for devices which detect or send electromagnetic radiation via an antenna structure and for the electrodes of transistors. Another application area where highly conductive structures are needed is to boost the current transport capacities of transparent electrodes with their rather high intrinsic sheet resistances in large area optoelectronic devices. Printing conductive inks is therefore an important part of solution processed electronics, and several studies have been published presenting work on R2R processing. An overview is presented in Table 2. In a very early example, Mäkelä et al. have employed a conductive polymer, which was R2R gravure printed on polypropylene substrates, followed by R2R nanoimprinting to achieve patterns with submicron resolution.<sup>[101]</sup> Processing speeds varied between  $0.2$  and  $1.0 \text{ m min}^{-1}$ , and while the specific volume conductivities achieved ( $3 \text{ S cm}^{-1}$ ) were quite modest, for a number of applications, this value might already be sufficient. A much more common method to prepare highly conductive structures, however, is to print them using metal based conductive inks. Several types of inks for a wide range of printing techniques are available, based on metalorganic decomposition (MOD) complexes, metal nanoparticles, micron sized metal flakes, or combinations thereof. For an in-depth overview of conductive inks, their formulation and chemistry,

**Table 1.** Deposition techniques, substrates, coating speeds, and TCM performances of R2R coated silver nanowire films.

Deposition and post-deposition technique (if applicable)	Substrate	Coating speed [ $\text{m min}^{-1}$ ]	Sheet resistance [ $\Omega \text{ sq}^{-1}$ ]	Transmission at 550 nm [%]	S2S application example	Reference
R2R slot die (mixture with PEDOT:PSS)	PET	2–10	>40	78	Electro-luminescent panel	[87]
R2R rod coating, then R2R solvent spraying, R2R compression rolling, immersion in salt solution and washing in water	PET and PEN	Not rep.	5	92	OFET, OLED, OPV	[90]
R2R rod coating	PET	Not rep.	38.3	Not rep.	OLED	[93]
R2R gravure, then laser welding	PET	1.5	5 and 13	91 and 95	None	[89]
R2R gravure, overcoating with graphene oxide dispersion (also multilayer stacking), then cold welding	PET	1.5	17	93	Flexible supercapacitor	[96]
R2R slot die (mixture with PEDOT:PSS)	PET	2.7	75	>90	None	[88]
R2R rod coating	PET	1.2	10 and 22	84 and 90	Electro-chromic device	[91]
R2R slot die (mixture with CNT)	Not rep.	2.0	102	87	None	[97]
R2R rod coating, then patterned photonic flash sintering (S2S) and R2R wiping of unexposed material	Poly-carbonate	2.0	17–18	ca. 80	OLED and transparent heater	[94]
R2R slot die, then overcoating with protective layer	PET	0.02	30–70	89–90	Touch panel	[92]
R2R rod coating, then R2R overcoating with UV resin, PET lamination, curing and peeling	PET	0.6	5	80	None	[95]
R2R printing (exact process not specified)	PET	2.0	46	87	Touch panel	[98]
R2R slot die	PET	1.0–10.0	32–94	86–92	OPV	[99]
R2R slot die (mixture with PEDOT:PSS), then R2R overcoating for planarization	PET	0.3	8–85	69–96	Perovskite PV	[100]

**Table 2.** Deposition and annealing techniques, substrate and ink types, printing speeds, and performance of R2R printed conductive structures.

Deposition and annealing technique	Substrate	Ink type	Printing speed [m min <sup>-1</sup> ]	Minimum feature size [μm]	Maximum Conductivity [S m <sup>-1</sup> ]	Reference
R2R inkjet, photonic flash sintering	PEN	Ag nanoparticle ink	10.0	<50	$7.6 \times 10^6$	[28]
R2R (rotary) screen, thermal (70–120 °C)	PES	Ag particle inks	6–10	200	Ca. $3 \times 10^6$	[119]
R2R flexo, thermal (80 °C)	PET	PA coated PMMA particles	15.25	40	50	[120]
R2R gravure, thermal (150 °C)	PET	Ag paste	2–8	20	Not rep.	[121]
R2R gravure offset, laser sintering (532 nm)	PET	Ag nanoparticle ink	0.6	N/A	$10.0 \times 10^6$ (value est. from $R_{sq}$ , $d$ , and ink composition)	[116]
R2R gravure, thermal (hot air oven)	PI	Ag flake paste	2.0	45	$6.25 \times 10^6$ (300 °C), $19 \times 10^6$ (400 °C)	[122]
R2R gravure, thermal (150 °C)	PET	Ag nanoparticle ink	5.0	13	Not rep.	[123]
S2S inkjet, R2R IR	PEN	Ag nanoparticle ink	0.07–2.0	N/A	$9.45 \times 10^6$	[124]
R2R (rotary) screen, thermal (140 °C), then R2R calendaring	PET	Ag flake paste	1.0	N/A	$4.5 \times 10^6$	[117]
R2R (rotary) screen, thermal (140 °C)	PET	Ag nanoparticle paste	2.0	90	Not rep.	[125]
R2R (rotary) screen, thermal (140 °C)	PET	Ag flake pastes	2.0	125	Up to $6.6 \times 10^6$	[126]
R2R gravure (150 °C)	PET, PEN	Ag nanoparticle ink	Not rep.	Not rep.	$3.0 \times 10^6$	[54]
R2R (rotary) screen, thermal (140 °C)	PET	Ag flake paste	10.0	Not. rep.	$2.1 \times 10^6$	[31]
R2R IJP, thermal (140 °C)		Ag nanoparticle ink	2.0		$53 \times 10^3$	
R2R flexo, thermal (140 °C)		Ag nanoparticle ink	10.0		$6.2 \times 10^6$	
R2R blade and gravure printing, thermal (curing not specified)	PET	Ag flake and nanoparticle pastes	4.0	N/A (full area)	$7.3\text{--}7.8 \times 10^5$	[127]
R2R IJP, thermal (140 °C)	PET and barrier film	Ag nanoparticle ink	2.0	132	$3 \times 10^6$	[128]
R2R flexo, thermal (140 °C)		Ag nanoparticle ink	25.0	133	$3.4 \times 10^6$ (values est. from $R_{sq}$ , and grid geometry)	
R2R gravure, thermal (80 and 150 °C)	PET and PI	Ag flake paste	0.5–10.5	121	$6.5 \times 10^5$	[129]

the reader is referred to a number of excellent reviews and book chapters dedicated to this topic.<sup>[102–104]</sup>

A number of key performance characteristics can be defined for conductive structures, which are the line width or more generally the feature resolution, the height and surface roughness of the structures, and the achieved electrical conductivities. For example, in cases where the metal lines serve to enhance the sheet resistance of transparent conductive materials, a narrow line width is preferred in order to retain as much transparent surface as possible.<sup>[105]</sup> Obviously, this situation requires a compromise in line dimensions and overall conductance, which can be shifted toward smaller structures only by increasing the specific conductivity. Three studies dedicated to the line width optimization and the ink transfer for the R2R gravure printing of silver nanoparticle inks on PET film have been published by Nguyen et al.<sup>[30,106,107]</sup> At line speeds of 2–10 m min<sup>-1</sup>, the authors obtained lines as narrow as 21 μm and demonstrated that air nip pressure and ink viscosity were the factors determining the line width, whereas for the height of the printed structures, the inks viscosity alone was dominant. Too high conductive structures, however, are not preferred in many cases, because coverage over a steep step can disturb the uniform and continuous deposition of subsequent functional layers, be it from solution or by dry techniques. To overcome this

issue, van de Wiel et al. have developed a method for embedding high and rough (several micrometers) printed silver structures into substrates by R2R techniques, thereby producing very flat films (surface roughness <5 nm) without sacrificing the high conductivity.<sup>[108]</sup> Instead of optimizing the printing conditions and ink formulations, Zhang et al. have demonstrated that the line width can also be narrowed down in the R2R gravure printing of silver nanoparticle inks at 4 m min<sup>-1</sup> by using printing rolls with miniaturized gravure cells (**Figure 5**).<sup>[109]</sup> In this case, line widths down to 19 μm and overall transmissions of the PET substrate of above 80% were obtained, although no values for the electrical characteristics of the structures were reported. The effect of various flexo printed grid geometries of silver ink patterns on the sheet resistance reduction of PET coated with ITO has been studied by Deganello et al.,<sup>[110]</sup> employing a web speed of 5 m min<sup>-1</sup>. At 18% surface coverage, these authors were able to reduce the sheet resistance from 45 Ω sq<sup>-1</sup> (ITO only) to 1.3 Ω sq<sup>-1</sup>. In a similar study published later by the same group, the track widths and mesh sizes of the silver grid were varied, and they managed to reduce this value further to 0.9 Ω sq<sup>-1</sup> at again 18% surface coverage.<sup>[111]</sup> At higher coverage (30%), even sheet resistances below 0.4 Ω sq<sup>-1</sup> were achieved, although these films will suffer from a very significant reduction in overall transparency. Using various



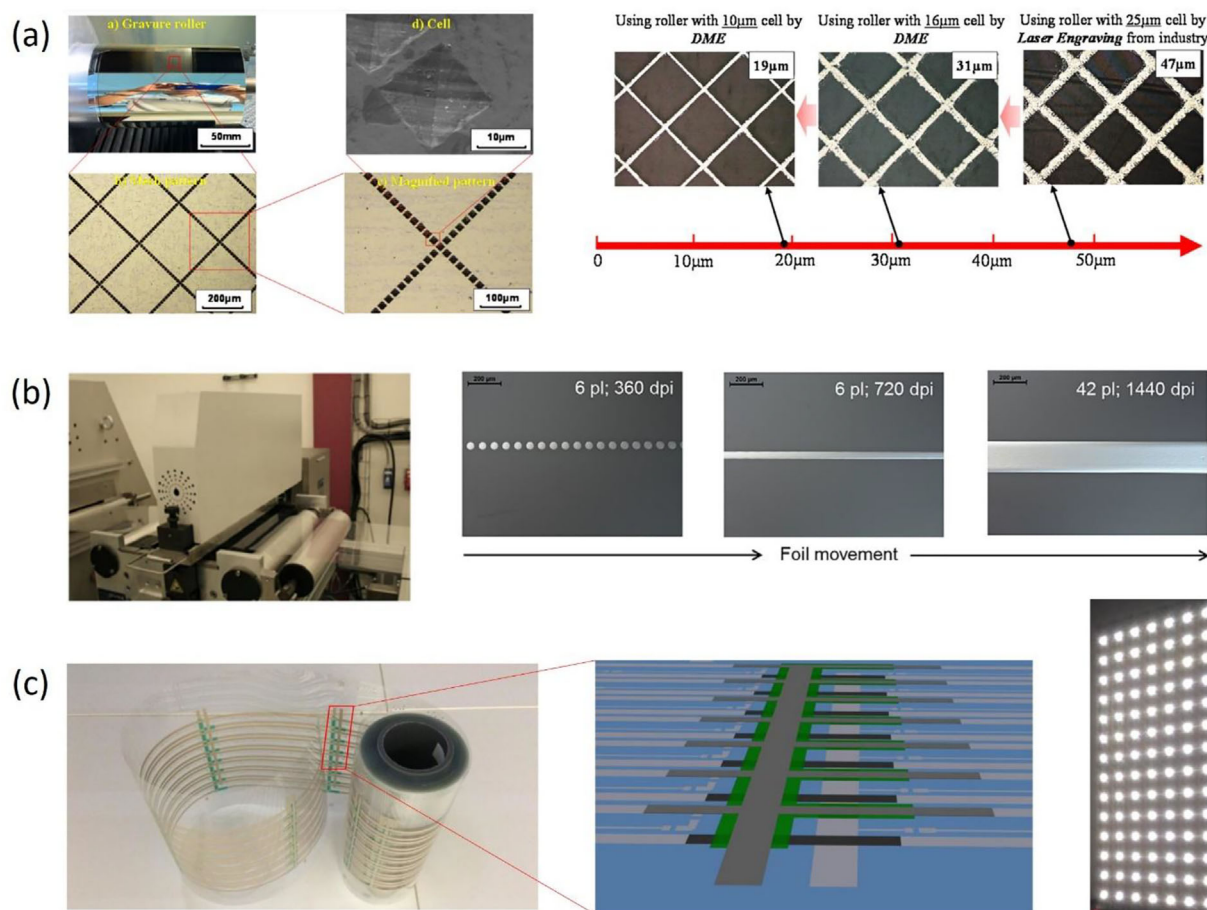


**Figure 5.** Production of electrically conductive structures by R2R printing of silver based inks. a) R2R gravure printing of nanoparticle ink: Gravure roll and details of the cells (left) and grid structures printed with different line widths (right). Reproduced with permission from ref. <sup>[109]</sup>. Copyright 2015 Elsevier. b) R2R inkjet printing of nanoparticle ink: Experimental setup (left) and silver lines printed using different droplet densities (right). Reproduced with permission from ref. <sup>[28]</sup>. Copyright 2014 IOP Science. c) Multilayer rotary screen printing of micrometer sized flake paste and a dielectric: Roll of foil with printed structures (left), design detail (center), and demonstrator with bonded LEDs (right). Adapted with from ref. <sup>[131]</sup> with permission. Copyright 2015 Springer Verlag.

silver salt solutions instead of nanoparticle based inks, Shin et al. have achieved similar results by R2R gravure printing, although neither the substrate nor the processing speed are mentioned.<sup>[112]</sup> In their case, sheet resistances of  $1\text{--}30\ \Omega\text{sq}^{-1}$  were reached at line widths down to  $20\ \mu\text{m}$  and overall transparencies of 85%, and the sheet resistances could actually be reduced further to  $0.3\text{--}0.4\ \Omega\text{sq}^{-1}$  when the silver traces were treated with a procedure called “blackening” by the authors. A similar system based on a mixture of silver oxide particles and silver salts has been formulated into a paste by Chun et al., R2R bar coated on PET as a thick film and thermally converted to a conductive silver layer with conductivities of up to  $2 \times 10^5\ \text{S cm}^{-1}$ .<sup>[113]</sup>

Whereas after deposition on the substrate, most functional electronic inks are simply cured by drying and/or chemical crosslinking, metal based conductive inks typically need more extensive post-deposition treatment in order to develop a proper electric conductivity suitable for the application. Particle based inks must be sintered for proper connectivity, whereas MOD inks require a chemical decomposition into elemental metal. Although this can be achieved in most cases by thermal

treatment, the time scales needed are frequently so long that their applicability for R2R processing at acceptable web speeds is limited. More than for other functional electronic inks, a number of post-deposition treatment alternatives to traditional oven drying have therefore been described in literature. Among these are photonic flash (also known as intense pulsed light) sintering, laser, microwave, electric, and chemical sintering. Their operating principles have been described in detail in several reviews.<sup>[114,115]</sup> All these techniques serve to accelerate the formation of highly conductive, dense metallic structures without damaging the underlying substrates, which, in the case of polymer films, are sensitive to elevated temperatures. Most studies have demonstrated the applicability only on a S2S basis; only a few have used R2R techniques. Of these, Abbel et al. demonstrated a strategy to scale up the inkjet printing and photonic flash sintering of silver nanoparticle inks from small scale S2S tests to R2R processing on a pilot production line at speeds up to  $10\ \text{m min}^{-1}$  (Figure 5).<sup>[28]</sup> At line widths of  $50\ \mu\text{m}$  and below, conductivities up to 12% of the bulk silver value were obtained on PEN substrates. Yeo et al. employed laser sintering

to post-process R2R gravure offset printed silver nanoparticle inks on PET at  $0.6 \text{ m min}^{-1}$  and achieved ca. 16% of the bulk silver value.<sup>[116]</sup> An alternative approach to improve the conductivity of R2R printed metal structures is calendaring, which has been demonstrated not only to increase the electrical conductance by 40–45%, but also to reduce surface roughness by 45–72%, depending on the paste used.<sup>[117]</sup> In other cases, initially R2R printed metal lines were further electroless plated with copper, again with the goal to increase the current transport capacity of the resulting structures.<sup>[118]</sup>

Printed current collecting grids are also important components of R2R solution processed solar cells, which will be discussed in detail in an own section of this review.

Where more complicated electrical wiring than only for power connection and distribution is required, multilayers of conductive structures must frequently be printed and electrical contacts at the crossing points must be prevented. For that reason, isolator layers are needed which must be deposited on top of the conductive lines with good registration accuracy to ensure the absence of short circuits and enable proper device functionality. Noh et al. have investigated and optimized the overlay accuracy of R2R gravure printed silver and dielectric inks on PET substrates at a web speed of  $12 \text{ m min}^{-1}$  for electrode applications.<sup>[130]</sup> They observed a marked difference of the registration accuracy between the web movement direction ( $41 \mu\text{m}$ ) and perpendicular to it ( $16 \mu\text{m}$ ), highlighting the importance of proper web handling to obtain functional features with high resolution. While a lot of attention has been spent in this study on the dimensions of the printed structures (line widening, film thickness, edge definition, and surface morphology) as a function of the inks' viscosities and the printing speed, no values for the conductivity were reported. A similar product, albeit with lower resolution, has been prepared by Keränen et al., who used R2R screen printing of silver paste and a UV curable dielectric at  $2 \text{ m min}^{-1}$  on PET (Figure 5).<sup>[131]</sup> In their case, a stack of silver/dielectric/silver was produced that was used as a wiring pattern to drive R2R assembled LED arrays. Also Yi et al. have studied the R2R gravure printing of silver nanoparticle pastes on PET film at  $6 \text{ m min}^{-1}$  and the subsequent overprinting of the resulting conductive structures with a dielectric  $\text{BaTiO}_3$  ink, also by R2R gravure printing, but at varying speeds of 4, 6, and  $8 \text{ m min}^{-1}$ .<sup>[132]</sup> Their key focus was on the optimization of the printing parameters for the dielectric ink to result in smooth and defect-free dielectric layers, and they demonstrated that the aspect ratio of the ink cells in the gravure roll is the dominant factor in this respect.

## 7. Light Emitting Devices

Light emission from electronic devices can be achieved using a number of physical processes, resulting in a variety of device architectures, all of which have in common that they require a complex stack of various functional materials, some of which need to be deposited as a continuous homogeneous film, whereas others must be structured. The working principles of light emitting electrochemical cells (LECs<sup>[133–137]</sup>), electroluminescent devices using alternating voltage (AC-EL<sup>[138]</sup>), and organic light emitting diodes (OLEDs<sup>[139,140]</sup>), have been

described in detail and therefore will not be explained here again. All these devices need some type of transparent electrode structure and highly conductive wiring, which has been discussed already in the two sections above. Here, we concentrate on the electronically functional layers in between these electrodes and their deposition by R2R techniques.

A major driver for the R2R production of light emitting devices is the production upscaling toward industrial mass manufacturing and cost reduction. Using the example of flexible LECs, Sandström et al. have both demonstrated the R2R production of these devices and provided a detailed cost calculation, which shows that this technology has the potential to be particularly competitive once high-throughput and high-volume production modes can be applied.<sup>[5,141]</sup> In their example, a PET film with ITO and zinc oxide was slot die coated with the emitting layer (a mixture of a conjugated polymer, poly(ethylene oxide) and a salt) and PEDOT:PSS at a speed of  $0.6 \text{ m min}^{-1}$ , resulting in a maximum brightness of  $150 \text{ cd m}^{-2}$  and a maximum efficacy of  $0.6 \text{ cd A}^{-1}$  (Figure 6). Comparing several case studies, some of which are still hypothetical at the current state of technology, the authors demonstrated that the transition from small scale S2S production toward high-volume R2R processing ( $60 \text{ m min}^{-1}$ ) could reduce the total cost down to  $11 \text{ € m}^{-2}$ , which represents an improvement of several orders of magnitude compared to the S2S approach. A similarly impressive reduction was predicted for the cost-per-lumen, where the most optimistic scenario resulted in only  $0.0036 \text{ lm €}^{-1}$ , albeit at an assumed luminance of  $1000 \text{ cd m}^{-2}$ .

R2R blade coating can be used to produce AC-EL panels, as has been demonstrated by Sunappan.<sup>[127]</sup> In this example, the main focus was on the deposition of the silver top electrodes, where blade coating and gravure printing were compared, but also the other functional layers (phosphors and dielectrics) were deposited by blade coating at  $4 \text{ m min}^{-1}$  on ITO coated PET film (Figure 6). When driven at 400 Hz and a voltage of 100 V, the devices emitted bluish light with a brightness in the range of  $250 \text{ lm m}^{-2}$ .

A more common device structure for light emission than LECs or AC-EL panels is the OLED, for which already in 2007, an approach has been proposed to enable the production of fully solution processed devices by R2R techniques, although, in practice, it was at the time still demonstrated by S2S spin coating only.<sup>[142]</sup> In order to prevent the technical problems associated with cathode deposition by metal evaporation on top of an organic stack, the authors employed a strategy in which two “half-fabricates” were prepared which upon lamination formed a complete OLED device. Starting from PET coated with ITO and aluminum, respectively, the “anode side” and the “cathode side” of the OLED were solution processed separately and only combined in a last step. In addition to avoiding evaporation on top of the organics, an additional advantage, especially for more complicated device structures, could be that interactions between already dried films and the still wet inks printed on top to deposit the next functional layer (redissolution, intermixing, improper wetting etc.), are partially circumvented. OLEDs prepared using this approach performed better than reference devices built up by a “hybrid” method, that is, a combination of (S2S) solution processing and evaporation, which was attributed to avoiding the damaging effects of Al evaporation on top of the organic layers.

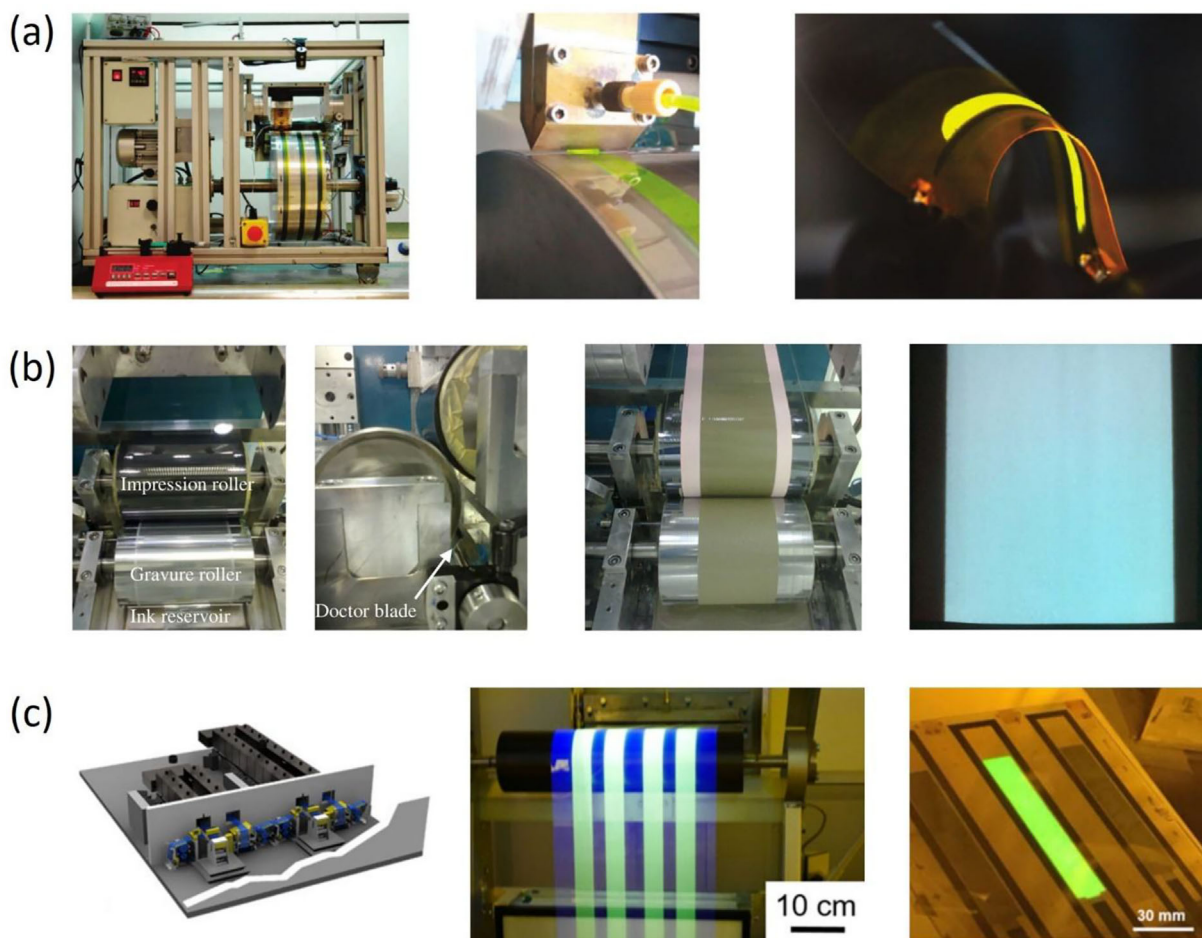


**Figure 6.** R2R solution processing of light emitting devices. a) Light emitting electrochemical cells by R2R slot die coating: Coating line (left), stripe coating of the active layer (center), final device (right). Reproduced with permission from ref. <sup>[141]</sup>. Copyright 2012 Nature Publishing Group. b) AC-driven electroluminescent panels by R2R blade coating: coating drums (left), coating of the silver electrode (center), final device (right). Reproduced with permission from ref. <sup>[127]</sup>. Copyright 2016 IEEE. c) Light emitting diodes by R2R slot die coating: Schematic representation of the coating line (left), stripe coating of the emissive layer (center), final device (right). Reproduced with permission from ref. <sup>[38]</sup>. Copyright 2017 Materials Research Society.

In 2013, Hast et al. presented a strategy to proceed from the small scale testing to the R2R pilot fabrication of OLEDs, starting with a PET roll with ITO patterns prepared by R2R etching.<sup>[143]</sup> The authors reported the R2R gravure printing of PEDOT:PSS and metal oxides, serving as the hole transport material, followed by the light emitting polymer, which was deposited using the same technique. The devices were then finished by rotary screen printing of an Al paste which acted as the top electrode, although the alternative of evaporating barium or calcium and then silver were also tested. The web speeds at which these processes were conducted were not revealed. Top encapsulation was achieved by the R2R lamination of a barrier film and the reported efficacies were in the order of  $3\text{--}5\text{ cd A}^{-1}$  with operational lifetimes (LT50) of 700–2500 h. Several application examples for the produced OLEDs were also demonstrated, such as smart packaging, smart cards, OLED indicators, and lighting or signage.

In the same year, R2R “cohesive coating” was demonstrated by Shin et al., where all functional OLED layers were deposited using a slot die coating setup, which however operated without

active ink pumping; instead, the ink flow was initiated and sustained by the web movement.<sup>[144]</sup> Starting with a PET substrate, two different types of PEDOT:PSS serving as both anode and hole injection layer were coated and resulted in films with sheet resistances of  $90\text{ }\Omega\text{ sq}^{-1}$  and transparencies of 83% at 550 nm. On top of this, the emissive layer, zinc oxide nanoparticles as the electron transport material and a PEO/salt mixture for electron injection were deposited. The flow rates and thus indirectly the layer thicknesses were controlled by the surface chemistry of the slot die. Again, no web speeds for the coating process have been reported. In the finished OLEDs, brightnesses exceeding  $10\,000\text{ cd m}^{-2}$  were achieved and maximum efficacies of up to  $6.1\text{ cd A}^{-1}$ , which was comparable to reference devices on glass/ITO. No information on lifetime data was reported.

More recently, R2R slot die coating at web speeds up to  $30\text{ m min}^{-1}$  for the hole injection materials and emissive polymer inks has been demonstrated using substrates of barrier films with ITO and metal structures which were spliced into longer rolls for ease of processing (Figure 6).<sup>[38]</sup> Using a R2R

processing line comprising two coating stations and drying ovens coupled to each other, the authors were able to coat both layers in a single run, using the so-called “tandem coating” approach. Furthermore, the special web handling system employed completely avoided top contact during substrate transport and coating, thereby eliminating a significant source of contamination and damage. After the coating process, the devices were cut out of the rolls and finished by S2S cathode evaporation, resulting in efficacies of  $5\text{--}7\text{ cd A}^{-1}$  at  $100\text{ cd m}^{-2}$  and operational lifetimes (LT50) of several hundred hours. In addition, it was demonstrated that by using appropriately prepared coating equipment, the active layers can also be deposited in a well-defined patterned manner by stripe coating (in the web direction) and intermittent coating (perpendicular to the web direction), which is important for the production of fully encapsulated OLEDs without pathways for side leakage for moisture, oxygen or other agents which shorten the devices’ shelf lives.

## 8. Photovoltaics

Of the very diverse materials systems which have been used for photovoltaic applications, those based on OPV and metal halide perovskites are particularly suited for deposition from solution. For detailed reviews of their materials chemistry, operating principles, deposition techniques, device architectures and related issues for S2S processing, the reader is referred to the existing literature.<sup>[145–149]</sup> Both types of solar cell materials systems have the potential for inexpensive mass fabrication by R2R manufacturing on flexible substrates and offer a wide choice of materials for applications where form factor and color are important. While OPV has undergone significant development already for some time, perovskite PV has very recently attracted a lot of attention.

### 8.1. Organic Photovoltaics

The main objectives in the field of OPV are achieving high efficiency, long term stability, and cost reduction. Low cost production can be reached by combining inexpensive materials with solution based R2R manufacturing techniques. Indeed, compared to conventional silicon based solar cells, organic solar cells are expected to be less expensive and easier to manufacture, due to lower energy consumption, low temperature and vacuum-free deposition, and the possibility of direct patterning during the coating process.<sup>[150,151]</sup> Thus, R2R coating and printing of organic semiconductors are the focus of many companies and research groups. Many different deposition techniques have been utilized and optimized for the production of thin functional layers of organic semiconductors and for OPV in particular.<sup>[152–154]</sup> Organic solar cells and modules with inkjet printed,<sup>[155,156]</sup> slot die coated,<sup>[157]</sup> spray coated,<sup>[158]</sup> gravure,<sup>[159]</sup> and flexographic<sup>[160]</sup> printed layers have been successfully demonstrated on S2S scale. Although S2S deposition has been proven to be compatible with industrial manufacturing, R2R techniques are still considered as the more preferred way for mass production, due to the promises of lower cost, higher throughput and

improved yield. Despite this, S2S approaches are still very important and can be considered as an intermediate step toward future R2R manufacturing. The knowledge generated by S2S scale experiments often serves as a support for R2R process development and optimization. For example, large area S2S slot die coated organic solar cells produced on flexible substrate from non-halogenated solutions<sup>[157]</sup> provide valuable input for R2R manufacturing, because halogen-free formulations are a decisive need for processing on industrial scales. After S2S demonstration, a further step toward production upscaling by R2R techniques is often the use of table top mini roll coaters.<sup>[161,162]</sup> These simple and low cost solution processing systems allow a direct investigation of the effects of variable R2R process settings on the resulting thin film quality. They have great potential to define reasonable starting values of parameters such as ink composition, coating speed or wet film thickness for subsequent R2R experiments on larger scale. Organic solar cells and modules manufactured using simple roll-coating systems for deposition of one or several functional layers have been demonstrated by several research groups.<sup>[163,164]</sup>

A pioneer of R2R OPV manufacturing is the group of Krebs at the Technical University of Denmark, DTU.<sup>[152,153,165–167]</sup> Krebs et al. have demonstrated numerous R2R processes for organic solar cell modules, with different device stacks employing different deposition methods.<sup>[152,153]</sup> In the so-called “Process One”,<sup>[167]</sup> OPV modules were manufactured on PET substrates coated with ITO. The first three layers (zinc oxide, the photoactive layer (PAL) and PEDOT:PSS) were processed using slot die coating. The silver back electrode was flat-bed screen printed to finalize the stack before it was laminated with barrier film for encapsulation. Since then, numerous variations of solar cell and module production based on this method have been published by the Danish group.<sup>[168,169]</sup> The first demonstrations were performed with P3HT:PCBM as a photoactive blend and then the process was further adapted for other photoactive materials.<sup>[170–172]</sup> Calculating the contributions of the various materials used in “ProcessOne” to the total cost of the embodied energy revealed that the ITO electrode is very expensive and forms a bottleneck for the price per watt peak.<sup>[173]</sup> Consequently, a number of ITO-free approaches were developed and demonstrated using R2R manufacturing.<sup>[128,165,166,174–176]</sup> These device architectures relied on ITO replacement by PEDOT:PSS<sup>[165]</sup> or silver current collection grids in combination with PEDOT:PSS.<sup>[128,174,175]</sup> Different printing methods were employed for the deposition of the front and back electrode grids.<sup>[31,177]</sup> The solar cell technology known as “IOne”<sup>[178]</sup> reported by DTU represents a significant progress in the all-solution and vacuum-free R2R manufacturing of organic photovoltaics (Figure 7). Compared to “ProcessOne”, “IOne” presents no disadvantages as it employs neither vacuum deposition nor does it rely on ITO. However, “ProcessOne” operates at lower materials and overall cost, is significantly faster and in addition yields devices with much better operational stability.<sup>[179]</sup> It should be noted that the “IOne” process has even been demonstrated in a silver-free version with only a carbon based electrode which showed the same performance as the version containing silver, thus indicating that neither ITO nor metal grids are required to prepare efficient and scalable OPV cells.<sup>[176]</sup> The efficient replacement of silver was achieved with



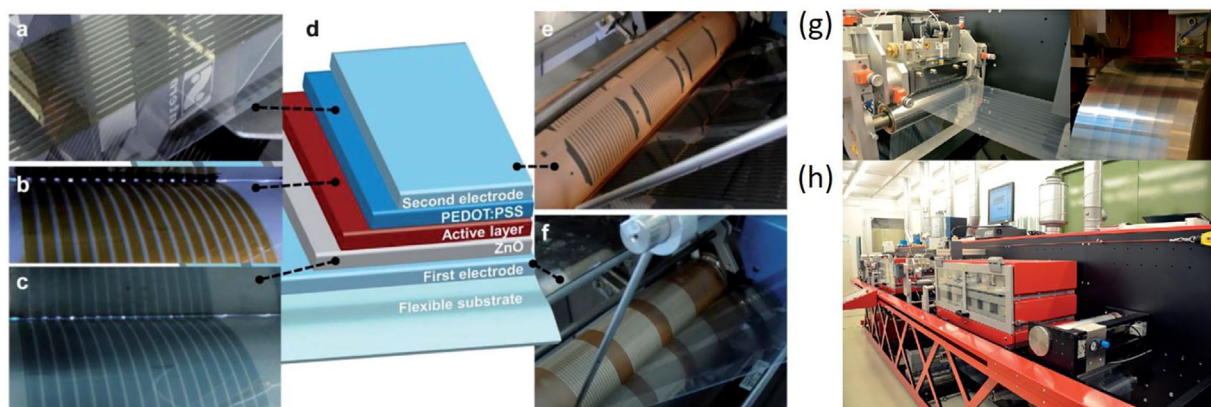


**Figure 7.** The device structure d) centrally surrounded by photographs of the R2R coating and printing processes, with a) and f) showing the rotary screen printing of the top and bottom PEDOT:PSS layers, respectively. c) and b) showing the slot die coating of zinc oxide and P3HT:PCBM, respectively, while e) shows the rotary screen printing of the graphite second electrode. Reproduced with permission from ref. <sup>[178]</sup>. Copyright 2012 Royal Society of Chemistry. One of the coating stations on the pilot line and the coating head of the MRC g), and the whole pilot line h). Reproduced with permission from ref. <sup>[187]</sup>. Copyright 2015 Wiley.

carbon paste, which yields superior printing and stability performance over printed silver conductors while requiring somewhat thicker printed layers to achieve the same conductivity.

Their great experience in the R2R deposition of different OPV materials allowed Krebs et al. to demonstrate the scalable R2R manufacturing of encapsulated large area, flexible organic tandem solar cell modules in ambient atmosphere (Figure 7).<sup>[180]</sup> Later, they successfully transferred a number of R2R deposition technologies for OPV manufacturing based on slot die coating of the main functional layers combined with printed electrodes, to the start-up company InfinityPV,<sup>[181]</sup> whose core business is printed electronics and printed organic solar cells in particular.

R2R slot die coating was also utilized by several other research groups worldwide for the manufacturing of the various layers in OPV cells and modules. Scientists from the Institute of Nuclear Energy Research in Taiwan employed this technique for the deposition of the electron transport layer (ETL) and the PAL for the production of inverted polymer solar cells (PSC).<sup>[182,183]</sup> Because their laboratory scale equipment (Figure 7) is not suited for full R2R processing, the PET/ITO substrates with the two R2R coated layers were cut into pieces and the devices were finished by S2S thermal evaporation of the hole transport layer (HTL) of MoO<sub>3</sub> and the silver electrodes. The systematic investigation of thermal effects during the drying step as well as the effect of thermal annealing on the film morphology and performance of inverted polymer solar cells fabricated by R2R slot die coating has been reported by Huang et al.<sup>[183]</sup>

A research group from the University of Newcastle has demonstrated a pathway for ITO-free fully R2R processed organic solar cells in a conventional geometry with a R2R sputtered aluminum top electrode.<sup>[184]</sup> This shows that solution processable printing and coating methods can be combined with R2R vacuum techniques for the manufacturing of complete OPV modules.<sup>[185,186]</sup>

Fully R2R slot die coated all-organic solar cells were produced and characterized by Andersson.<sup>[187]</sup> The manufacturing process is exclusively based on inexpensive components, benign solvents

and materials with a low environmental impact. The coating was performed on FOM Technologies' Solar X3 R2R inline coating and printing machine, which is equipped with a sticky roller web cleaning unit, a preheating oven, and two complete slot die coating stations, each having a 1 m long double pass (2 m drying distance) horizontal hot air-drying oven and a preceding corona unit (Figure 7). One of the main problems of the reported devices was a predisposition for short circuits. Mechanical failures in the active layer due to swelling of the bottom electrode material during processing have been identified as the reason for this phenomenon. Although the performance of the OPV devices did not exceed 1%, this study emphasized the important notion that the mechanical properties of the constituent layers and their interfaces are perhaps even more critical than the electro-optical properties of the active layer, which currently attracts the clear majority of the research efforts when it comes to large scale production.

Most of the slot die coated modules mentioned above were produced using stripe coating to allow the interconnection of individual cells in the modules. Because for optimal performance, the dimensions of single cells in the module should typically not exceed 1 cm,<sup>[188,189]</sup> the stripe coating technology typically provides quite low geometrical fill factors (GFF, the ratio between the active area and total area of the OPV module) in the range of 50–75%.<sup>[168,180]</sup> Laser interconnection can significantly reduce the dead area and seems to be more effective for OPV manufacturing, as it can provide high GFFs of up to 95%.<sup>[190]</sup> Holst Centre – Solliance has reported OPV modules prepared using three R2R slot die coated layers (ZnO/PAL/PEDOT:PSS; Figure 8) and either screen printed or inkjet printed back electrodes.<sup>[191]</sup> The interconnections in these modules were made by laser patterning, which provided a very high GFF of 92.5%. This approach of combining laser patterning of the coated layers and printing techniques for the deposition of the top electrodes is unique and was used to produce both non-transparent and semi-transparent modules from non-chlorinated solvents (Figure 8). A variety of halogen-free solvents were tested and compared, and the drying parameters optimized on



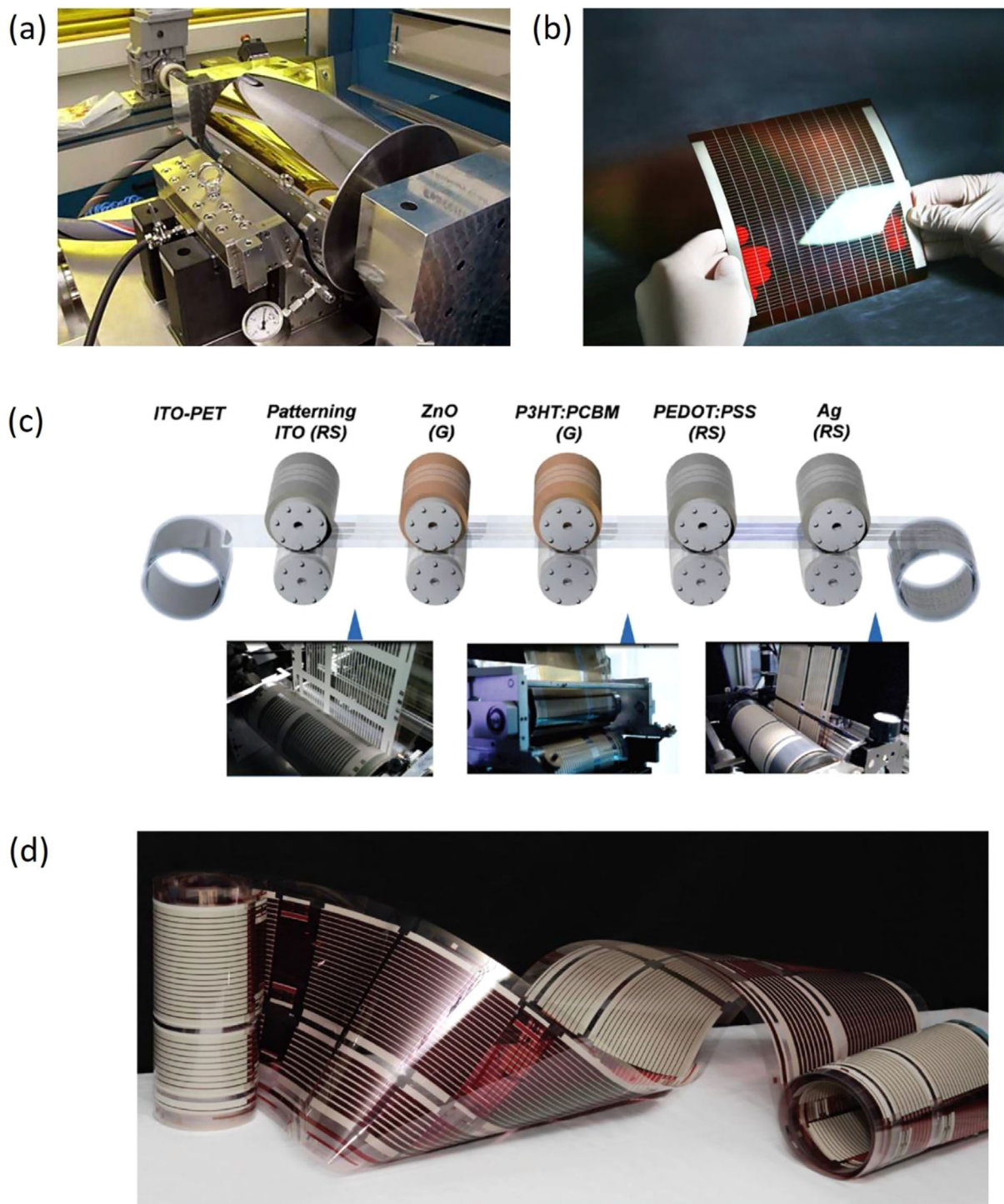


**Figure 8.** a) Slot die coating unit the R2R line at Holst Centre – Solliance. Reproduced with permission from ref. <sup>[192]</sup>. Copyright 2011 Elsevier. b) Semi-transparent OPV module with high GFF, R2R manufactured at Holst Centre – Solliance. Reproduced with permission from ref. <sup>[204]</sup>. Copyright 2015 Wiley. c) R2R process of printed inverted OPV modules at VTT. The used printing methods for separated OPV layers are abbreviated as RS (rotary screen printing) and G (gravure printing). d) R2R fabricated printed OPV modules made using the manufacturing process shown in c). Reproduced with permission from ref. <sup>[198]</sup>. Copyright 2015 Royal Society of Chemistry.

R2R scale in order to demonstrate the technology readiness for industrial large area manufacturing.<sup>[192]</sup>

The use of gravure and flexographic printing was also extensively investigated and has demonstrated their promise for the R2R preparation of organic solar cells.<sup>[159,193–200]</sup> These two-dimensional printing techniques are differentiated from other coating methods by enabling the direct patterning of arbitrarily shaped and sized features, thereby enhancing the freedom to connect the cells in modules. Prior to R2R processing on a full industrial scale, a lot of research has been done on smaller laboratory equipment.<sup>[159,201,202]</sup> Similar to S2S slot die coating, gravure printing carried out on lab scale equipment allows process parameter optimization and the identification of suitable ink properties in order to make the transition to the future full R2R process. Thus, up to four functional OPV layers have successively been S2S gravure printed on flexible PET substrates coated with ITO, enabling high production throughput in a R2R printing process.<sup>[193,194]</sup>

R2R pilot production of OPV modules has been realized by researches from VTT.<sup>[195,198–200]</sup> Starting from simple table top equipment, this group was able to transfer lab scale processes<sup>[196,197]</sup> to the R2R fabrication of OPV modules using gravure printing and rotary screen printing.<sup>[198]</sup> The fabrication process allows direct 2D patterning and resulted in the manufacturing of OPV modules with an active area up to 96.5 cm<sup>2</sup> (Figure 8). To further demonstrate the capability of the applied printing methods (gravure and rotary screen printing), a variety of designs was introduced and proven to work by the same research group.<sup>[199]</sup> Similar work has also been reported by the research group of Holst Centre who also demonstrated fully inkjet printed solar cells with arbitrary designs.<sup>[155]</sup>

Furthermore, as reported by teams at CSIRO and the University of Melbourne, partly and fully printed OPV modules have been fabricated using R2R reverse gravure deposition.<sup>[203]</sup> According to the authors, reverse gravure printing is similar to conventional gravure printing from a process point of view, but the films formed using either method differ strongly from each other.

Besides from academic research groups, the R2R manufacturing of solution processed OPV has also attracted a lot of interest from industry. Thus, without mentioning the contributions of companies working on this topic, a review on the recent developments in this field would not be complete.

Eight19's solar cell technology is based on solution processable organic semiconductor materials, which are processed into solar cells using continuous R2R printing and coating processes.<sup>[205]</sup> Based on technology originally developed by the Cavendish Laboratory at the University of Cambridge, Eight19's technical team has designed and optimized a versatile R2R coating plant capable of producing up to 200 000 m<sup>2</sup> of OPV annually. OPVIUS GmbH (formerly BELECTRIC OPV) develops and manufactures organic solar cells and focuses on the commercialization of customized OPV solutions.<sup>[206]</sup> Armor Group is a French company specialized in R2R printing and produces OPV films on an industrial scale under the ASCA<sup>®</sup> tradename.<sup>[207]</sup> The ability to produce films of various standards that range from 5 to 12 V equivalent modules reflects the flexibility and agility in their industrial facilities.<sup>[208]</sup> The industrial machines designed and used by ARMOR allow to

move from a standard mode of production for OPV (one layer by one coating pass) to a simultaneous coating process. By the end of 2017, Armor will be able to produce up to 24 V equivalent OPV modules with a total production capacity of 1 million square meters. Organic solar cell modules manufactured by CSEM Brasil reached the level of rapid prototyping<sup>[209]</sup> and their scaling up laid the base to co-found SUNEW in 2015.<sup>[210]</sup> SUNEW is an OPV production pilot line of 35 m divided in five stations with a capacity to produce 35 000 m<sup>2</sup> per month. InfinityPV ApS is a Danish start-up company founded in 2014 by Frederik C. Krebs along with 31 co-owners.<sup>[181]</sup> InfinityPV's flexible OPV modules can be prepared entirely using R2R printing and coating techniques. The production is based on solution processing of all the layers at low temperatures and ambient conditions and the process is therefore highly energy efficient and ensures a short energy payback time compared to most of the existing inorganic solar cell technologies. The technology does not include toxic or scarce elements and is, therefore, environmentally safe.

Although many successful examples of the integration of R2R coated and printed OPV modules have been demonstrated,<sup>[169,211–213]</sup> including the installation of OPV-based solar parks (Figure 9),<sup>[213]</sup> there are still many issues which need to be resolved before full scale commercialization of these technologies can seriously start.<sup>[214,215]</sup> An important issue in the manufacturing of OPV concerns the environmental impact of the various process steps. Indeed, typical solvents used for the photoactive materials are halogenated aromatic solvents, for example, chlorobenzene or ortho-dichlorobenzene. OPV devices show the highest performance when produced using these solvents. Driven by environmental concerns and the potential commercialization of OPV technologies, several groups have demonstrated highly efficient OPV modules produced from non-halogenated solvent using R2R compatible techniques.<sup>[157,192,216]</sup> Often changing a solvent composition can lead to significant changes in the morphology of the photoactive layer,<sup>[192]</sup> which is composed of two materials (donor and acceptor). The optimal bulk heterojunction morphology and thereby high PCE is determined by factors like domain size (optimum is ca. 10 nm), domain purity, interfacial width between the domain,<sup>[217,218]</sup> and the crystallinity of the phases,<sup>[219]</sup> especially in the case of crystalline polymers, such as P3HT. Apart from the solvents used for the deposition of the photoactive layer, the morphology can be controlled by the drying and annealing process,<sup>[220,221]</sup> the ratio between the donor and acceptor and by the properties of the layer underneath. Many studies performed in the past focused on the morphology optimization of the photoactive layer<sup>[222,223]</sup> and on transferring these findings to R2R manufacturing,<sup>[163,222]</sup> where a lot of efforts are directed toward quality control strategies for the printed layers.<sup>[179,224]</sup> The layer quality analysis during the coating and a better prediction of whether the module will work or fail can significantly increase the yield of the produced modules and therefore lower manufacturing costs.

The next important parameters which will bring the OPV technology closer to full scale commercialization are a high GFF, which already has been demonstrated in R2R coated modules<sup>[191]</sup> and the freedom of forms, as has been demonstrated with inkjet printing<sup>[155]</sup> or gravure printing.<sup>[199]</sup> The remaining issues hampering mass production and full commercialization

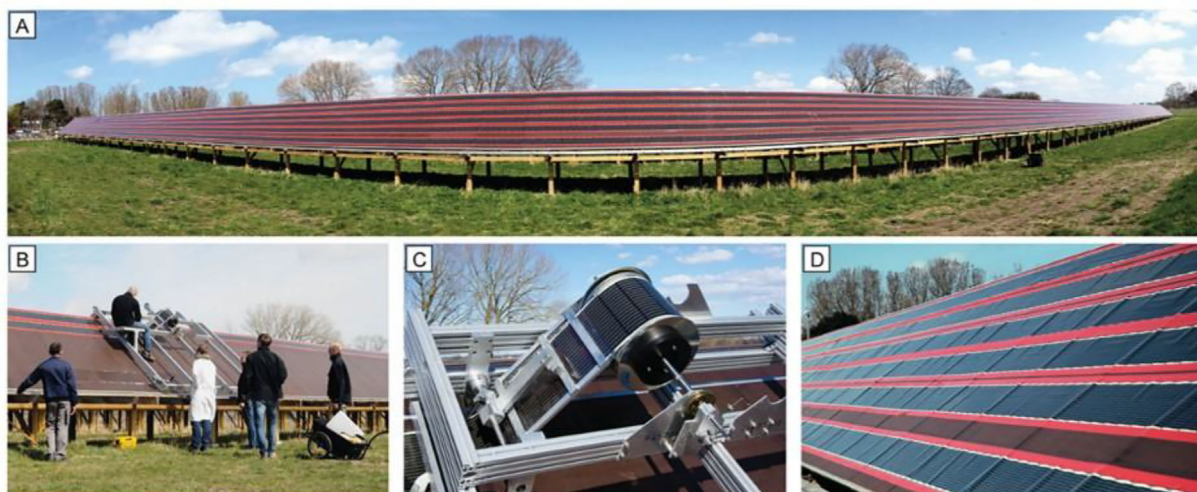


**Figure 9.** a) The front row of the solar park with six lanes of 100 m stretches of solar cell foil with a web width of 305 mm. b) Roll mounting of the foil along with c) a close-up photograph of the application with a guide. d) A view along the row showing dilation around connections in the platform. Reproduced with permission from ref. <sup>[213]</sup>. Copyright 2014 Wiley.

of OPVs are the still relatively low power conversion efficiencies<sup>[225]</sup> and insufficient stability.<sup>[226,227]</sup> Efficiency is becoming an increasingly important driver for reducing the cost of large area PV systems.<sup>[228]</sup> Solving these issues will open a lot of new perspectives for organic solar cells.

## 8.2. Perovskite Photovoltaics

The interest in perovskite PV has significantly increased over the last few years.<sup>[229–232]</sup> High power conversion efficiencies (PCE) and the potentially low cost make it a very promising candidate for future applications.<sup>[233,234]</sup> Rapid progress in research and development has been demonstrated in recent years. The certified record efficiency of perovskite solar cells has already reached 22.7%,<sup>[235]</sup> making this approach competitive with traditional silicon technologies. Although many issues such as stability, toxicity or current–voltage (I–V) hysteresis need to be resolved before the commercialization of this technology can commence, scale-up and large area processing have already become the focus of the latest research.

The active area of perovskite PV reported in the literature is mostly limited to few a square millimeters. The scale-up of the active area of the devices is expected to lead to an efficiency drop due to the series resistance of the electrodes.<sup>[236]</sup> Theoretical modeling performed by Galagan et al. revealed the critical influence of the electrode sheet resistance on the performance of perovskite solar cells and modules when scaling up the active area of the sub-cells.<sup>[237]</sup> Simulated results show that if the sheet resistance of one of the electrodes (e.g., the transparent conducting oxide) is  $10 \Omega \square^{-1}$ , the optimum width of the sub-cells in the module is in the range of 0.3–0.7 cm, while the usage of ITO on foil limits this value to only 0.3 cm. These results identified several critical issues in the large area processing and scaling up of perovskite PV technology. First, because the width of the sub-cells in the modules is relatively small, the efforts should be focused on reducing the interconnection (dead) area.

Laser technology seems to be most promising to achieve a high aspect ratio between the active area and the interconnections zone.<sup>[238]</sup> Thus, many reports were dedicated to the manufacturing of perovskite PV modules,<sup>[239–243]</sup> however, most of these studies used spin coating for the deposition of the layers.

In order to move from the lab scale toward industrially compatible manufacturing, in analogy to the successful experience with organic solar cells, many printing and coating techniques have been adapted for the preparation of perovskite PV cells. Because different layers in the perovskite devices have different physical properties, the selection of deposition methods must be guided by similar considerations as in OPV to optimize each layer in the device stack. For example, screen printing was often utilized for the deposition of mesoscopic  $\text{TiO}_2$  and  $\text{Al}_2\text{O}_3$  materials,<sup>[243,244]</sup> while inkjet printing was successfully applied for the deposition of nanocarbon based hole extraction layers.<sup>[245]</sup> The first attempts to replace spin coating for the processing of the perovskite layer were done using blade coating.<sup>[246–249]</sup> Although this is not strictly a R2R deposition method, it can be considered as an intermediate step for further scale-up. This technique has been widely used for the fabrication of organic solar cells and proven to be a simple, environmentally friendly and low-cost method for solution processed photovoltaics.

High throughput ultrasonic spray coating was used for the fabrication of the perovskite layer, whereby functional films with high uniformity, crystallinity and surface coverage were obtained in a single step.<sup>[250]</sup> In order to extend this process toward flexible plastic substrates, high temperature annealing (often required to cure the  $\text{TiO}_2$  layer) must be avoided. The photonic curing technique, which is compatible with the use of plastic substrates, was used for the annealing of the  $\text{TiO}_2$  layer. This technique enables the R2R high temperature processing of thin film materials on low temperature substrates. S2S screen printed triple layers of a mesoporous stack have been reported by several research groups.<sup>[251,252]</sup> Monolithic perovskite modules with dimensions of  $10 \times 10 \text{ cm}^2$ , an active area of  $70 \text{ cm}^2$  and 10.74%



efficiency, along with an outstanding shelf life stability, have been demonstrated by Priyadarshi et al.<sup>[251]</sup> Similarly, stable large area ( $10 \times 10 \text{ cm}^2$ ) printable mesoscopic perovskite modules exceeding 10% efficiency have also been prepared by Hu et al.<sup>[252]</sup> Weihua Solar has developed a slot die coating process combined with a gas pumping method for fabricating compact large area perovskite layers. After annealing of the perovskite film, a carbon layer was screen printed on top which acts as a collector for positive charges and back contact. Then the deposited layers were laser scribed into several strips, forming the series connections. Based on these techniques, Weihua Solar showed they can produce large area perovskite modules from  $5 \times 5$  to  $45 \times 65 \text{ cm}^2$ . The power conversion efficiencies for the  $5 \times 5 \text{ cm}^2$  modules reached 10.6% with good reproducibility.<sup>[253]</sup>

Significant progress in the upscaling of perovskite solar cells using slot die coating has also been demonstrated by several research centers and academic groups.<sup>[89,253–257]</sup> Krebs et al. reported the device manufacturing on flexible substrates using scalable techniques such as R2R slot die coating under ambient conditions.<sup>[254]</sup> Printing the back electrodes using both carbon and silver was essential to the success of the scaling effort. Both normal and inverted device geometries were explored, and it was found that the formation of the correct morphology for the perovskite layer depends heavily on the surface upon which it is coated, and this has significant implications for manufacturing. A significant loss in performance of around 50% was found when progressing to a fully scalable fabrication process; this observation is comparable to what has been frequently found for other printable solar cell technologies such as OPV. The PCE for devices processed using spin coating on ITO coated glass with an evaporated back electrode yielded a PCE of 9.4%. When devices of the same device type with identical area were realized using slot die coating on flexible ITO/PET with a printed back electrode, the PCE dropped to 4.9%.<sup>[254]</sup> This approach was further developed by DTU in collaboration with Zhejiang University, where a self-assembled monolayer deposited onto PEDOT:PSS modified the crystallinity and coverage of the perovskite film, resulting in a much smoother surface morphology.<sup>[89]</sup> This improved the PCE from 3.7% to 5.1% in flexible perovskite devices deposited by slot die coating using roll-coating equipment. Printed perovskite solar cells were

demonstrated also with slot die coating as a scalable printing method by Hwang et al.<sup>[255]</sup> A sequential process was developed to produce efficient perovskite PV devices which can be used in a large scale R2R printing process. Devices in which all layers except the electrodes were printed demonstrated a PCE of up to 11.96%, confirming that perovskite solar cells can be effectively produced by R2R processes.

Solliance and its research partners focus on using scalable, industrial processes toward the fabrication of large area solar cell modules, which will eventually be suitable for seamless integration in a broad variety of PV systems. First, using S2S slot die coating, Solliance has demonstrated  $168 \text{ cm}^2$  perovskite modules with 10% efficiency,<sup>[258]</sup> and later the result was improved to 13.75% on the aperture area (or 14.5% on the active area).<sup>[259]</sup> Twenty four cells were serially connected through optimized P1, P2, P3 laser interconnection technology, demonstrating the scalability of the new thin film perovskite PV technology. The results were further explored toward scalability using R2R technologies. The in-line R2R coating, drying and annealing processes were executed at a linear speed of  $5 \text{ m min}^{-1}$  on a 30 cm wide commercial PET/ITO foil under ambient conditions (**Figure 10**). Solliance has achieved the world record PCE of 13.5% level for perovskite-based photovoltaics using industrially applicable, R2R production processes,<sup>[260]</sup> which is an improved result compared to the previously reported value of 12.3%.<sup>[257]</sup> Modules produced by R2R demonstrated a PCE of 12.2% for  $10.5 \text{ cm}^2$  on the aperture area (active area efficiency of 13.5%) and a PCE of 10.1% for  $160 \text{ cm}^2$  modules (active area efficiency of 11.1%; **Figure 10**). All process steps on the R2R line were performed using low cost materials while keeping the process temperatures below  $120^\circ\text{C}$ . The Solliance team states that this capability shows the high volume production potential of this emerging thin film PV technology.

## 9. Transistors and Logic

The general device structure of organic thin film transistors (TFT) and their physical working principles have been described in a number of reviews<sup>[261,262]</sup> and will therefore not be explained here in detail. A frequent approach is to print the gate, source,

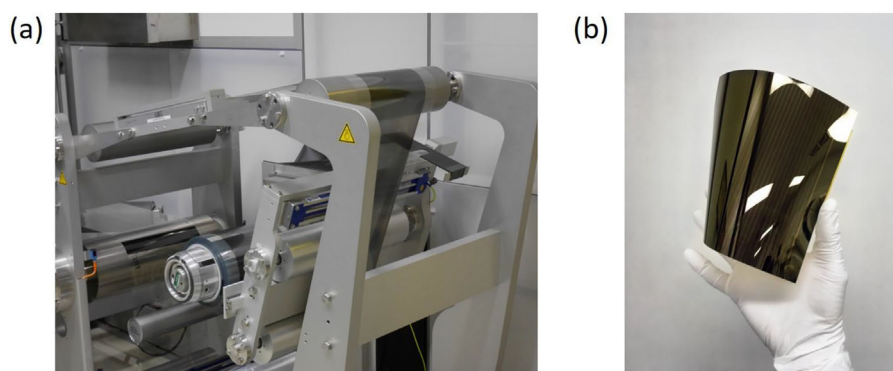


**Figure 10.** a) Perovskite layer slot die coated on Solliance's R2R line. Reproduced with permission from ref. <sup>[257]</sup>. Copyright 2017 Solliance. b) R2R produced flexible perovskite PV module with aperture area of  $160 \text{ cm}^2$  and PCE of 10.1%. Reproduced with permission from ref. <sup>[260]</sup>. Copyright 2017 Solliance.

and drain electrodes using metallic inks, in a very similar manner, as described in the section on printed electric connections. Furthermore, insulating and dielectric materials are also needed, all of which have also been deposited by R2R solution techniques. For the channel materials, a wider variety of different R2R printable semiconductor materials has been used. One particularly interesting application area for R2R printed TFTs is smart packaging, where low product prices are a key element for commercial success<sup>[263]</sup> and which has been reviewed by Jung et al.<sup>[4]</sup> A very early paper on the R2R coating and printing of some materials relevant for organic TFTs has been published by Klink et al. already in 2005, but the layer quality they obtained was insufficient to actually produce working devices, which had to be demonstrated by receding to S2S deposition techniques.<sup>[264]</sup> More recently, particularly Cho's research group has driven the development forward by an impressive output of publications, most of which focused on their system of R2R gravure printed silver, barium titanate and carbon nanotubes on PET films (**Figure 11**). Although as for the OLED and OPV applications, most of the published work is based on polymer films, paper substrates have also been successfully used for R2R printed OTFTs.<sup>[265]</sup> In contrast to applications such as OLEDs and OPV, where a trend toward increasingly large device areas is evident, miniaturization is a typical feature in the field of printed transistors. As a consequence, high resolution and good registration accuracy methods are needed and several studies have addressed these issues. For example, Nguyen et al. have developed a model for ink spreading during R2R gravure printing on flexible substrates and experimentally optimized printing parameters for a silver nanoparticle ink and achieved line widths of 20  $\mu\text{m}$  when a high viscosity ink was used (**Figure 11**).<sup>[121]</sup> For gravure printed layers, Noh et al. have achieved registration accuracies of 40  $\mu\text{m}$ ,<sup>[266]</sup> and a similar value of 50  $\mu\text{m}$  has been reported by Park et al. who employed the same deposition technique.<sup>[267]</sup> In a more recent report, this value was improved to 20  $\mu\text{m}$  by Koo et al., making use of a camera-controlled alignment system on their R2R gravure printing line (**Figure 11**).<sup>[268]</sup> A comparable method has also been developed by Kim et al. to measure the registration error in R2R multilayer prints, using the input from a camera detection system installed on the printing line.<sup>[269]</sup> Scalability of production processes is another important issue, which was investigated by Yi et al., who optimized a number of R2R gravure printing and drying parameters (web speed, cell geometry, drying temperature) for silver nanoparticle based conductive and  $\text{BaTiO}_3$  based dielectric inks. Their primary goal was to optimize layer thicknesses and surface morphology and device yields for the capacitors of 100% were reported.<sup>[132]</sup> A decisive materials property for the printed semiconductor materials is their charge carrier mobility, whereas the transistor devices themselves are typically characterized by their on/off ratio. In a very recent paper, mobilities of up to  $0.21 \text{ cm}^2 \text{ Vs}^{-1}$  and on/off ratios of about  $10^6$  have been reported.<sup>[270]</sup> In most cases, however, significantly lower numbers are obtained, as can be seen in **Table 3**, which provides an overview about the literature on R2R printed TFTs and their performances. A detailed discussion of the challenges which the mass production of printed TFTs still faces, is provided by Noh et al., who point out that the accuracy and reliability of current printing techniques still poses

significant limitations on a widespread commercial use.<sup>[271]</sup> One challenge is electrode overlap due to insufficient alignment control, which causes parasitic capacitances and thus reduces the transistors' switching speeds. Vilkman et al. have therefore developed a self-alignment concept for electrode production which is a hybrid approach of R2R printing and lithography.<sup>[272]</sup> Printing first a graphic sacrificial ink (R2R flexo printing at  $10 \text{ min}^{-1}$ ) on PET, silver was subsequently evaporated uniformly and selectively washed away by removal of the underlying ink at  $0.3\text{--}0.5 \text{ min}^{-1}$  in a solvent bath, giving a substrate with the gate electrodes, capacitor bottom electrodes and electrical wiring. R2R reverse gravure printing of PMMA ( $8 \text{ min}^{-1}$ ) was then applied to deposit the dielectric layer and in a following step, positive photoresist was R2R flexo printed as stripes, cured by illumination through the substrate (at  $10 \text{ min}^{-1}$ , employing the gate electrode as the photomask for source and drain) and developed by etching ( $2 \text{ min}^{-1}$ ). A second sacrificial resist could be R2R flexo printed op top ( $10 \text{ min}^{-1}$ ) to directly pattern the capacitor top electrodes and top wiring, because registration is less critical for these. After homogeneous silver evaporation and lift-off for both resists simultaneously, the semiconductor was R2R reverse gravure printed ( $4 \text{ min}^{-1}$ ). Using this self-aligned approach, the authors were able to demonstrate electrode registration accuracies below 5  $\mu\text{m}$ .

## 10. Sensors

Another highly important application area of R2R printed electronics is sensor devices, which have been reported based on a number of highly various physical principles. A recent overview about substrates, materials, and (S2S and R2R) printing technologies used for printed electronics with a particular focus on sensing applications is provided by Khan et al.<sup>[20]</sup> One common approach, mainly put forward by the group of Cho, is to combine R2R printed transistors with sensing devices and RFID antennas for easy read-out.<sup>[263,267,276–279]</sup> One of their prime motivations for R2R printing is manufacturing cost reduction, which is quantitatively supported by a study by Zhiquan et al., who developed a configurable model for cost and resource consumption for such processes and demonstrate it using the example of a printed RFID tag on PET, also identifying additional options for further materials use and cost reduction.<sup>[282]</sup> A first step into this direction was taken with the demonstration of a fully printed 1-bit radiofrequency tag containing a rectifier, based on PET substrates with R2R gravure printed antennas, wiring, TFT electrodes, and dielectrics and inkjet printed carbon nanotubes.<sup>[263]</sup> After S2S pad printing of resistors using a carbon ink, inverters, and ring oscillators were obtained with oscillation frequencies in the range from 1 to 60 Hz at 10 V. These were finished into complete rectennas by S2S pad printing of a mixture of polyaniline and zinc oxide nanowires as the semiconductor element and aluminum paste for the top electrodes. The final devices had a reading distance of 2 cm. Although in this study, all processing steps after the R2R printing of the transistors were carried out by S2S pad printing, the authors argued that these could straightforwardly be replaced by R2R gravure printing. Using a slightly adapted materials system, the same research group succeeded in doing so two years



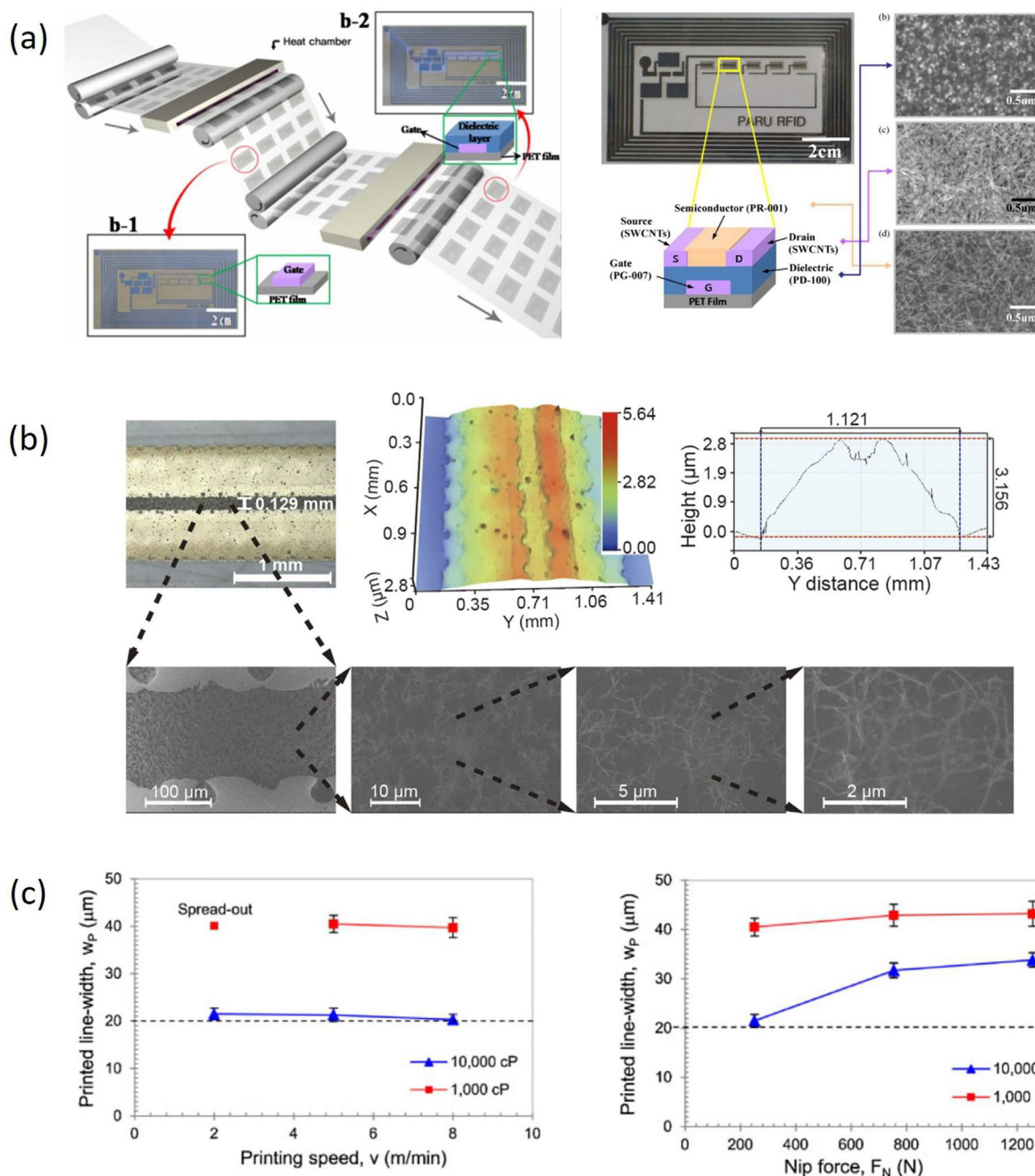


**Figure 11.** a) R2R printing for TFT production: schematic representation of the production process (left), device architecture (center) and SEM images of the different printed materials (right). Reproduced with permission from ref. [263]. Copyright 2010 IEEE. b) Multilayer R2R printing of TFT inks (silver, barium titanate, and carbon nanotubes) with high registration accuracy. Reproduced with permission from ref. [268]. Copyright 2015 Nature Publishing Group. c) Optimized R2R gravure printing of silver ink to obtain narrow conductive structures for TFT applications: Line width dependence on printing speed (left) and nip force (right). Reproduced with permission from ref. [121]. Copyright 2014 The Japan Society of Applied Physics.

later, when they demonstrated the first rectenna on PET film prepared completely by R2R gravure printing (Figure 12).<sup>[267]</sup> In this case, the process consisted of the subsequent deposition of the antenna and bottom electrodes using silver nanoparticle ink, then dielectric ( $\text{BaTiO}_3$ ), and insulator (epoxy) deposition, zinc oxide printing for the active layer, followed by diode top electrode deposition (Al paste). The devices were finished by printing the

wiring and the capacitor top electrodes, again using Ag nanoparticle ink. All layers were processed by R2R gravure printing at a speed of  $8 \text{ m min}^{-1}$ , and the device yield was above 90%. Thus, produced rectennas were demonstrated to be able to convert 5 V AC into 4.0–4.5 V DC voltage at a frequency of 13.56 MHz and a reading distance of 2 cm. In subsequent research, it was shown that similar R2R printed TFT substrates

**Table 3.** Deposition techniques, substrates, processing speeds, and performance of R2R prepared TFTs.

Deposition techniques	Substrate	R2R Printing Speed [ $\text{m min}^{-1}$ ]	Mobility [ $\text{cm}^2 \text{Vs}^{-1}$ ]	On/off ratio	Device Yield [%]	Reference
R2R blade coating, R2R screen printing	Metallized PET	Not reported	Not reported	Insufficient layer quality for device production by R2R processing	0	[264]
R2R gravure printing	PET	0.5	$5 \times 10^{-4}$	<100	Ca. 75	[273]
R2R gravure printing, S2S Inkjet printing	PET	5.0	0.03–5.24	100–1000	Not reported	[263]
R2R gravure printing, S2S inkjet printing	PET	12.0	0.006–0.12	1000	Not reported	[274]
R2R gravure printing	PET	10.0	0.2–0.5	100–10 000 (depending on TFT design)	Not reported	[266]
R2R gravure printing	PET	8.0	Not reported	2500	>90	[267]
R2R inkjet printing, R2R flexo printing, R2R reverse gravure printing	Coated paper	10.0 (flexo)	Not reported	Not reported	Not reported	[265]
R2R screen printing, R2R slot die printing	Thin glass with patterned ITO	Not reported	Not reported	Not reported	Not reported	[275]
R2R gravure printing	PET	8.0	Not reported	Not reported	Ca. 80	[276]
R2R gravure printing, R2R rotary screen printing	Ag coated PET	7.0–10.0	0.017–0.026	100–1000	Not reported	[277]
R2R gravure printing	PET	6.0–8.0	Up to 0.23	Depending on channel length; 5200 for $130 \mu\text{m}$	>90	[268]
R2R gravure printing, Roll-to-sheet (R2S) gravure printing	PET	8.0	0.0028–1.43	Up to 300	Not reported	[278]
R2R gravure printing	PET	8.0	0.015–0.027	500–850	18–98, depending on TFT design	[279]
R2R gravure printing, S2S inkjet printing	PET	Not reported	>5	35 000	Not reported	[280]
R2R flexo printing, S2S slot die coating printing, S2S screen printing	PET	20	Not reported	100	Not reported	[281]
R2R flexo printing, R2R reverse gravure printing	PET	4.0–10.0	0.0016	1300	Up to 67	[272]
R2R gravure printing, R2S gravure printing, S2S inkjet printing	PET	10–25	0.21	1 000 000	Not reported	[270]

can be used to build electrochromic humidity sensors when a second functionalized polymer film was laminated on top.<sup>[276]</sup> This film had been prepared by R2R coating of a PEDOT:PSS layer, subsequent screen printing of PMMA to define a signage pattern, and finally coating of an electrolyte (PEO/LiClO<sub>4</sub> mixture). The finished device was able to display a predefined pattern selectively above a relative humidity of 70%. Using a similar approach, R2R printed silver patterns on PET were finished by R2S gravure printing and on top of these substrates, electrochemical cells were deposited, enabling the authors to detect a model analyte at a concentration of 10 mM (Figure 12).<sup>[278]</sup> Finally, also touch sensors with a resolution of 9 ppi have been constructed by laminating a pressure sensitive rubber on top of a fully R2R printed TFT active matrix.<sup>[279]</sup> Already earlier, a R2R processed touch sensor on a plastic substrate with a printed metal mesh of  $10 \mu\text{m}$  resolution has been reported, albeit without details about the processing conditions.<sup>[283]</sup>

A different approach has been chosen by Potyrailo et al., who started with a PET substrate fully coated with a thin film of aluminum on which a positive resist pattern was R2R printed and the non-covered aluminum subsequently etched away.<sup>[284]</sup>

Although the conductive structures have not been deposited by a printing technique in this case, R2R printing was thus nevertheless used to achieve their shape definition. After chip attachment, extruded films of the sensing material (PEUT) were laminated on top and the thus produced multivariant vapor sensors were able to selectively detect various organic volatile compounds at molar fractions down to 3%. A similar concept to produce electric wiring, though based on the R2R slot die coating of silver nanowire ink (at up to  $5 \text{ m min}^{-1}$ ) on PET and PI films, has been presented by Lee et al., who removed excess silver by R2R laser ablation.<sup>[285]</sup> The thus formed conductive silver structures were applied as a strain sensor and exhibited a gauge factor of 2.8.

For photodetectors, R2R microgravure printing has been applied to deposit methylammonium lead iodide perovskite precursor solutions on PET substrates at  $0.2 \text{ m min}^{-1}$ , which upon oven drying resulted in perovskite nanowire coatings with a high degree of orientation (Figure 12).<sup>[248]</sup> From these rolls, sheets were cut out and processed further by S2S evaporation techniques to yield photodetectors with a sensitivity of about 100 ( $I_{\text{light}}/I_{\text{dark}}$ ) at  $36 \text{ mW cm}^{-2}$  illumination and a photoresponsivity

of ca.  $2 \text{ mA W}^{-1}$ . Colorimetric oxygen sensors have been produced by R2R flexography of a mixture of methylene blue and  $\text{TiO}_2$  nanoparticles, which acted as a UV-A activated photocatalyst, at  $10 \text{ m min}^{-1}$ .<sup>[286]</sup> The authors also used reverse gravure printing at lower speeds,  $1.0\text{--}1.6 \text{ m min}^{-1}$ , and the produced sensors reversibly changed their cyan color density from 0.1 to 1.9 (reflectivity change from ca. 1% to ca. 80%) during exposure to normal atmospheric oxygen levels and simultaneous UV-A illumination. R2R flexographic coating of graphite pastes on paper at  $60 \text{ m min}^{-1}$  has been used to suppress the inherent luminescence from the substrate materials and to thus improve the sensitivity of sensors based on surface enhanced Raman scattering after liquid flame spray coating of silver nanoparticles on top.<sup>[11]</sup> Electrochemical biosensors have been prepared by the R2R flexo printing of

three functional layers (carbon electrodes, Ag/AgCl electrodes, and zinc oxide nanowire precursor) at rather low speeds ( $0.2\text{--}0.6 \text{ m min}^{-1}$ ) on polyimide substrates.<sup>[287]</sup> After appropriate functionalization of the nanowires with an enzyme and integration of pieces cut from the printed rolls, sensors could be prepared which were able to detect glucose down to a concentration of  $46 \mu\text{mol l}^{-1}$ . Capacitive humidity sensors on PET have been produced by rotary screen printing silver, isolator, and another silver layer, the performance of which had been improved by calendaring.<sup>[117]</sup> The calendaring procedure gave rise to a 10% increase in quality factor of the LC-circuit used in the sensor design, whereas the resonance frequency decreased somewhat. Flex sensors have been produced by R2R microgravure printing of composites of activated carbon and PVDF at rather low web speeds of  $18 \text{ cm min}^{-1}$  on PET films.<sup>[288]</sup> Stable

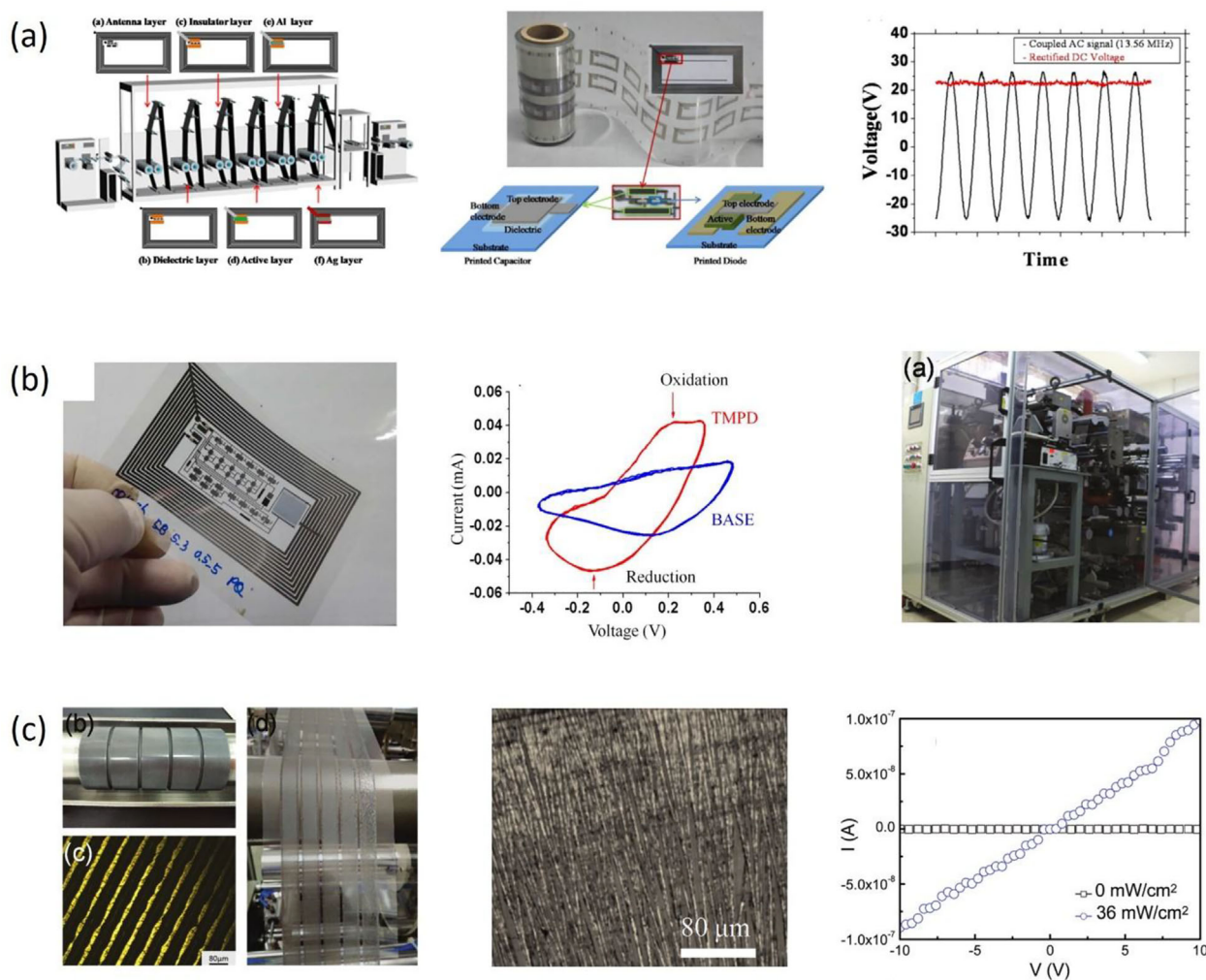


**Figure 12.** R2R printing for sensor production. a) Rectenna on PET film prepared completely by R2R gravure printing: Schematic representation of the printing line (left), roll of printed devices (center) and rectifier performance (right). Reproduced with permission from ref. <sup>[267]</sup>. Copyright 2012 IOP Science. b) R2R gravure printed electrochemical cells: Device image (left), cyclic voltammetry curves in the presence and absence of analyte (center) and R2R equipment used to prepare the sensors (right). Reproduced with permission from ref. <sup>[278]</sup>. Copyright 2015 Nature Publishing Group. c) R2R microgravure printing of methylammonium lead iodide for photodetector applications: R2R printing line (full overview and details) and printing of precursor material (left), SEM image of printed nanowire array (center), and IV characteristics with and without illumination (right). Reproduced with permission from ref. <sup>[248]</sup>. Copyright 2016 Royal Society of Chemistry.

and consistent changes in electrical resistance were observed when bending samples cut out of the roll up to 120° outwards and inwards. Applying an additional protective coating of PVAc, also by R2R microgravure printing, resulted in a similar sensitivity at reduced power consumption.

## 11. Emerging Applications

This final chapter serves to present a number of technical approaches for the R2R processing of electronic inks which are

still in a rather early stage of development and the industrial significance of which is still in the process of becoming apparent.

Guo et al. have developed a R2R line, which is equipped with a coating station (for blade and flow coating of dispersions of functional particles), an electric and magnetic alignment tool, a UV curing unit and a thermal gradient tool, which can operate at speeds between  $1.5 \text{ mm min}^{-1}$  and  $240 \text{ mm min}^{-1}$  (Figure 13).<sup>[289]</sup> Exposure to the electric or magnetic fields can result in the alignment of dispersed particles in the z-direction, that is, along the film thickness

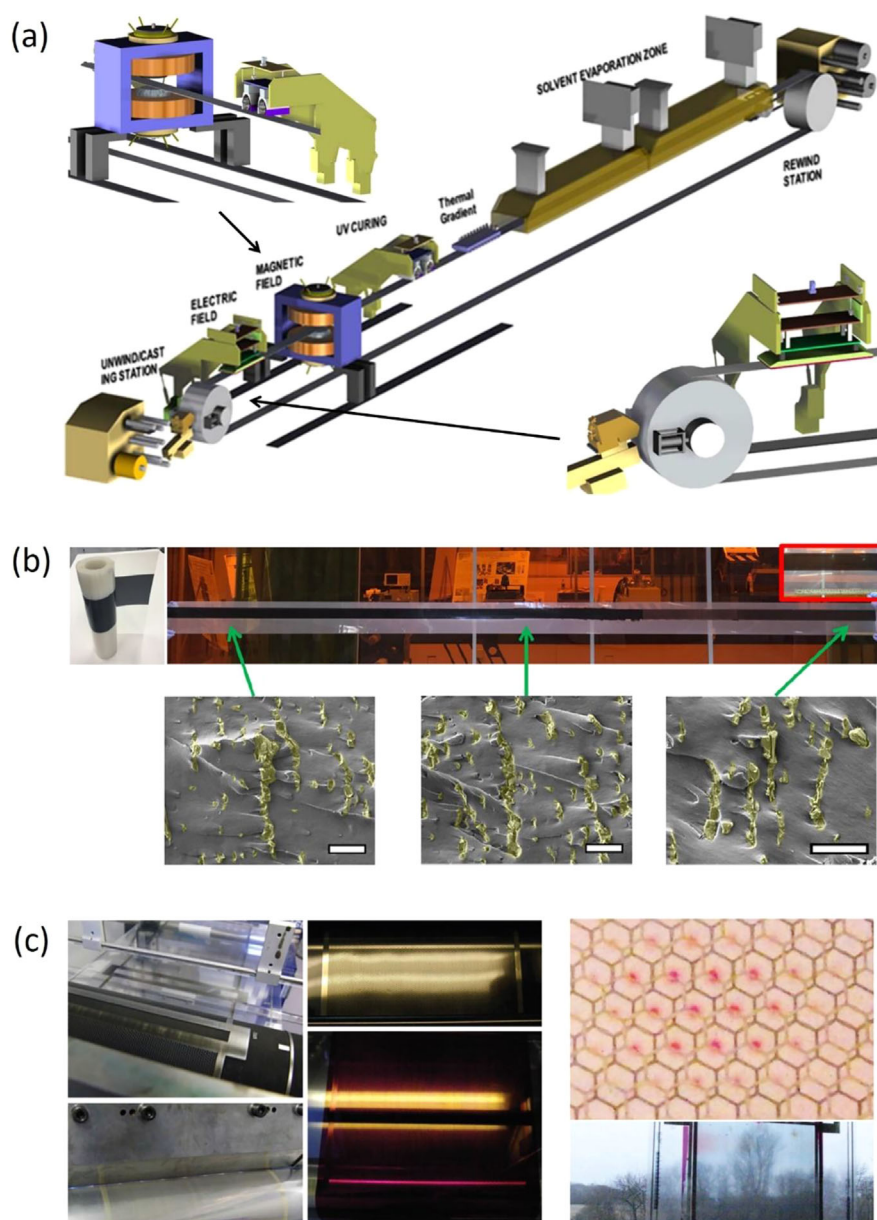


**Figure 13.** a) R2R line for the coating, alignment and curing of composite materials. Adapted from ref. <sup>[289]</sup> with permission. Copyright 2015 Wiley. b) Photograph of the R2R alignment of graphite flakes, with representative SEM images of samples taken from the roll. Reproduced with permission from ref. <sup>[293]</sup>. Copyright 2017 American Chemical Society. c) R2R coating of functional inks for electrochromic devices (left), close-up image of reduction of electrochromic dye (top right), and device photograph (bottom right). Reproduced with permission from ref. <sup>[295]</sup>. Copyright 2013 Wiley.



axis, which is then fixed by UV-induced or thermal cross-linking of the matrix. For a number of materials, this has resulted in films with strongly anisotropic properties, for which the authors foresee practical applications in a number of areas like capacitors, batteries, and sensors. For example, clay platelets, nickel nanowires, and BaTiO<sub>3</sub> nanoparticles have been subjected to R2R coating and alignment in this tool.<sup>[289–291]</sup> Using dispersions of nickel nanoparticles in siloxane, which could be R2R blade coated on a non-magnetic metal carrier, aligned by exposure to a magnetic field, and then thermally crosslinked, all at 0.05 m min<sup>−1</sup>, nickel columns were formed traversing the 200 μm thick film in the z-direction.<sup>[292]</sup> This caused piezoresistivity, where the electrical conductivity along the z-axis was improved by seven orders of magnitude under a pressure of 1–3 MPa, compared to non-aligned samples. Recently, the same authors showed that thick films (15 μm) of graphite flakes dispersed in siloxane, when exposed to an electric field opposite to the web direction, can be aligned in the z-direction (Figure 13).<sup>[293]</sup> The coating and alignment steps took place at 0.5 m min<sup>−1</sup>. By subsequent thermal curing of the siloxane monomers into PDMS rubber at very low web speed (10 mm min<sup>−1</sup>), the orientation was fixed and, for example, at 1 vol% graphite loading, films were obtained with highly anisotropic materials properties (ca. tenfold improvement of both electrical conductivity and dielectric permittivity in the z-direction, compared to a non-aligned film).

Prototype components for electronic textiles have been prepared by R2R dispensing one layer each of two different PEDOT:PSS formulations (two times 1 μm) on 5 mm wide PET ribbons, resulting in an overall sheet resistance of 34 Ω sq<sup>−1</sup>.<sup>[294]</sup> No processing speed was reported in this case. On top of this conductive coating, silicone drops were R2R dispensed and annealed, which subsequently were capped with two more PEDOT:PSS layers, such that electrical contact with the bottom conductive layer was made. These ribbons were then interwoven into a fabric with uncoated (and thus isolating) PET ribbons, resulting in a flexible fabric with a highly stable electric resistance upon bending.

In a similar approach as already known for large area solar cells, Søndergaard et al. have R2R flexo printed a silver nanoparticle based ink on PET films with a barrier coating to form current conductive grids (Figure 13).<sup>[295]</sup> Two of these electrode film rolls were R2R slot die coated with electrochromic and charge balancing components, respectively. The processing speed for all R2R steps was 10 m min<sup>−1</sup>. Sheets cut from the two rolls were finally assembled by S2S techniques with an ionic electrolyte layer in between and yielded flexible electrochromic panels with switching times similar to ITO-based reference devices.

Lo et al. have R2R flexo printed patterns on a PEN film using a sacrificial black ink, which then was full area R2R sputtered with Al and SiO<sub>2</sub> and finally, the ink was washed off, together with the Al and SiO<sub>2</sub> on it.<sup>[296]</sup> This resulted in a roll of conductive structures covered by an isolating layer with a resolution of ca. 100 μm. Spacers were then R2R gravure printed on top of this substrate using an adhesive mixed with black carbon pigments. Laminating another PEN film homogeneously covered with aluminum on top of this lower

substrate resulted in a microelectromechanical system (MEMS) which exhibited display functionality. Authors from the same group have later developed this concept further and patterned only the metal structures (silver instead of aluminum in this case) using their R2R method with sacrificial ink.<sup>[297]</sup> After washing off, the isolation layer was introduced by R2R gravure printing of a SiO<sub>2</sub>-based polysiloxane ink. The spacers were this time printed on the top electrode film (a PET roll with a homogeneous thin silver coating) and finally, the devices were finished again by R2R lamination. The entire R2R process could be carried out at a speed of 5 m min<sup>−1</sup>. Experimental flexible 3 × 3 active MEMS-controlled matrix displays with transmittances of ca. 50% were fabricated using this approach and demonstrated switchability between the three primary colors red, green and blue.

## 12. Summary and Conclusions

R2R printing and coating is a promising approach toward the industrial mass production of electronic devices for a number of commercially interesting applications. R2R processes are already well established in mass production for the media, packaging, and photographic industries, but their widespread use for electronics applications is still under development. The main benefits of R2R printing and coating include easy processing (no need for vacuum deposition) and the potential of low cost and high production yield. For rather simple technologies like smart cards, industry has already started to use R2R technologies. The production processes for more complicated devices like lighting elements, transistors or solar cells, however, still require some additional improvement before they can be successfully transferred to mass production. The decisive benefit of R2R printing and coating in the electronics industry is seen in lowering production costs. Therefore, inexpensive, ubiquitous low-end and potentially disposable devices are generally judged as the most promising application areas on the short term. By contrast, significant improvements are still needed in order to compete with vacuum based technologies and thus enter the high-end application markets. This additional progress is estimated to require several years of additional research in materials and process optimization. A particularly promising recent development is the tremendous progress made in the emerging field of perovskite solar cells. New efficiency records for devices produced by printing and coating are continuously being reported. As a consequence, the further development of a R2R solution manufacturing technology for perovskite solar cells is becoming one of the most active research areas in the field. Currently, the biggest challenges for R2R coated and printed electronics lie in the improvement of device yield, performance and reliability, and a further lowering of end product costs. If this is achieved, chances for a successful commercialization will improve tremendously with respect to the current situation.

## Conflict of Interest

The authors declare no conflict of interest.



## Keywords

coating, roll-to-roll, high-volume production, large-scale manufacturing, printing, solution processed electronics

Received: December 31, 2017

Revised: March 30, 2018

Published online: April 30, 2018

- [1] H. Kipphan (Ed.), *Handbook of Print Media*, Springer Verlag, Berlin, Heidelberg, Germany **2001**.
- [2] <https://www.energy.gov/sites/prod/files/2016/02/f30/QTR2015-6K-Roll-to-Roll-Processing.pdf>. Last accessed Dec 30, **2016**.
- [3] K. Wiesenhütter, W. Skorupa, in *Subsecond Annealing of Advanced Materials* (Eds: W. Skorupa, H. Schmidt), Springer International Publishing, Cham, Switzerland **2014**, Ch. 14.
- [4] M. Jung, J. Kim, H. Koo, W. Lee, V. Subramanian, G. Cho, *J. Nanosci. Nanotechnol.* **2014**, 14, 1303.
- [5] A. Sandström, L. Edman, *Energy Technol.* **2015**, 3, 329.
- [6] C. A. Bishop, *Vacuum Deposition onto Webs, Films and Foils*, William Andrew Publishing, Norwich, United States **2006**.
- [7] H. J. Park, L. J. Guo, in *Progress in High-Efficient Solution Process Organic Photovoltaic Devices*, Vol. 130 (Eds: Y. Yang, G. Li), Springer Verlag, Berlin, Heidelberg, Germany **2015**, Ch. 12.
- [8] J. E. Greene, *J. Vac. Sci. Technol. A* **2017**, 35, 05C204.
- [9] D. Garg, P. B. Henderson, R. E. Hollingsworth, D. G. Jensen, *Mater. Sci. Eng. B* **2005**, 119, 224.
- [10] V. Subramanian, J. B. Chang, A. de la Fuente Vornbrock, D. C. Huang, L. Jagannathan, F. Liao, B. Mattis, S. Moles, D. R. Redinger, D. Soltman, S. K. Volkman, Q. Zhang, *38th European Solid-State Device Research Conference*, Edinburgh, United Kingdom **2008**, 34, 17.
- [11] J. J. Saarinen, D. Valtakari, S. Sandén, J. Haapanen, T. Salminen, J. M. Mäkelä, J. Uozumi, *Nord. Pulp Pap. Res. J.* **2017**, 32, 222.
- [12] Y. Yamamoto, S. Harada, D. Yamamoto, W. Honda, T. Arie, S. Akita, K. Takei, *Sci. Adv.* **2016**, 2, e1601473.
- [13] M. B. Schubert, J. H. Werner, *Mater. Today* **2006**, 9, 42.
- [14] W. S. Wong, A. Salleo (Eds.), *Flexible Electronics - Materials and Applications*, Springer International Publishing, Cham, Switzerland **2009**.
- [15] S. Biswas, O. Shalev, M. Shtein, *Annu. Rev. Chem. Biomol. Eng.* **2013**, 4, 289.
- [16] N. Chen, D. H. Kim, P. Kovacic, H. Sojoudi, M. Wang, K. K. Gleason, *Annu. Rev. Chem. Biomol. Eng.* **2016**, 7, 373.
- [17] J. Park, K. Shin, C. Lee, *Int. J. Precis. Eng. Manuf.* **2016**, 17, 537.
- [18] G. Grau, J. Cen, H. Kang, R. Kitsomboonloha, W. J. Scheideler, V. Subramanian, *Flexible Printed Electron.* **2016**, 1, 023002.
- [19] C. Ru, J. Luo, S. Xie, Y. Sun, *J. Micromech. Microeng.* **2014**, 24, 053001.
- [20] S. Khan, L. Lorenzelli, R. S. Dahiya, *IEEE Sens. J.* **2015**, 15, 3164.
- [21] R. Abbel, E. R. Meinders, in *Nanomaterials for 2D and 3D Printing* (Eds: S. Magdassi, A. Kamyshny), Wiley-VCH, Weinheim, Germany **2017**, Ch. 1.
- [22] Y. Z. Ping, H. Y. An, B. N. Bin, W. X. Mei, X. Y. Lun, *Chin. Sci. Bull.* **2010**, 55, 3383.
- [23] A. A. Tracton (Ed.), *Coating Technology Handbook*, 3rd ed., CRC Press, Boca Raton, United States **2006**.
- [24] P. M. Schweizer, S. E. Kistler (Eds.), *Liquid Film Coating*, 1st ed., Springer Science and Business Media, Dordrecht, The Netherlands **1997**.
- [25] K. L. Jarvis, P. J. Evans, *Thin Solid Films* **2017**, 624, 111.
- [26] P. van de Weijer, P. C. P. Bouten, S. Unnikrishnan, H. B. Akkerman, J. J. Michels, T. M. B. van Mol, *Org. Electron.* **2017**, 44, 94.
- [27] E. K. Baumert, O. N. Pierron, *Appl. Phys. Lett.* **2012**, 101, 251901.
- [28] R. Abbel, P. Teunissen, E. Rubingh, T. V. Lammeren, R. Cauchois, M. Everaars, J. Valetton, S. van de Geijn, P. Groen, *Transl. Mater. Res.* **2014**, 1, 015002.
- [29] Y. Ishida, G. Nakagawa, T. Asano, *Jpn. J. Appl. Phys.* **2007**, 46, 6437.
- [30] H. A. D. Nguyen, C. Lee, K.-H. Shin, *Robot. Comput. Integr. Manuf.* **2017**, 46, 122.
- [31] M. Hösel, R. R. Søndergaard, D. Angmo, F. C. Krebs, *Adv. Eng. Mater.* **2013**, 15, 995.
- [32] R. R. Søndergaard, M. Hösel, F. C. Krebs, *J. Polym. Sci. Part B: Polym. Phys.* **2013**, 51, 16.
- [33] W. Clemens, D. Lupo, S. Kirchmeyer, K. Hecker, C. Ranfeld, *White Paper - OE-A Roadmap for Organic and Printed Electronics*, 7th ed., Organic and Printed Electronics Association, Frankfurt am Main, Germany **2017**, p. 95.
- [34] D. J. Coyle, in *Liquid Film Coating*, 1st ed. (Eds: P. M. Schweizer, S. E. Kistler), Springer Science and Business Media, Dordrecht, The Netherlands, **1997**, Ch. 12a.
- [35] C. K. Aidun, N. G. Triantafillopoulos, in *Liquid Film Coating*, 1st ed. (Eds: P. M. Schweizer, S. E. Kistler), Springer Science and Business Media, Dordrecht, Netherlands, **1997**, Ch. 12d.
- [36] H. G. Lippert, in *Coatings Technology Handbook*, 3rd ed. (Ed: A. A. Tracton), CRC Press, Boca Raton, United States **2006**, Ch. 19.
- [37] H. Kang, J. Park, K. Shin, *Robot. Comput. Integr. Manuf.* **2014**, 30, 363.
- [38] R. Abbel, I. de Vries, A. Langen, G. Kirchner, H. t'Mannetje, H. Gorter, J. Wilson, P. Groen, *J. Mater. Res.* **2017**, 32, 2219.
- [39] M. Schmitt, P. Scharfer, W. Schabel, *J. Coat. Technol. Res.* **2014**, 11, 57.
- [40] D. Maza, M. S. Carvalho, *J. Coat. Technol. Res.* **2017**, 14, 1003.
- [41] A. Reale, L. L. Notte, L. Salamandra, G. Polino, G. Susanna, T. M. Brown, F. Brunetti, A. D. Carlo, *Energy Technol.* **2015**, 3, 385.
- [42] M. Karakaya, J. Zhu, A. J. Raghavendra, R. Podila, S. G. Parler, J. P. Kaplan, A. M. Rao, *Appl. Phys. Lett.* **2014**, 105, 263103.
- [43] J. S. Chang, A. F. Facchetti, R. Reuss, *IEEE J. Emerg. Sel. Topics Circuits Syst.* **2017**, 7, 7.
- [44] V. Subramanian, J. Cen, A. de la Fuente Vornbrock, G. Grau, H. Kang, R. Kitsomboonloha, D. Soltman, H.-Y. Tseng, *Proc. IEEE* **2015**, 103, 567.
- [45] H. Kang, R. R. Baumann, *Int. J. Precis. Eng. Manuf.* **2014**, 15, 2109.
- [46] J. Lee, K. Shin, C. Lee, *Robot. Comput. Integr. Manuf.* **2015**, 35, 77.
- [47] J. Park, K. Shin, C. Lee, *Robot. Comput. Integr. Manuf.* **2014**, 30, 432.
- [48] J. Seong, S. Kim, J. Park, D. Lee, K.-H. Shin, *Int. J. Precis. Eng. Manuf.* **2015**, 16, 2265.
- [49] L. H. Rossander, H. F. Dam, J. E. Carle, M. Helgesen, I. Rajkovic, M. Corazza, F. C. Krebs, J. W. Andreasen, *Energy Environ. Sci.* **2017**, 10, 2411.
- [50] S. W. Jeon, C. Kim, C. H. Kim, *J. Mech. Sci. Technol.* **2015**, 29, 5069.
- [51] J. Chang, S. Lee, K. B. Lee, S. Lee, Y. T. Cho, J. Seo, S. Lee, G. Jo, K.-Y. Lee, H.-S. Kong, S. Kwon, *Rev. Sci. Instrum.* **2015**, 86, 055108.
- [52] C. Lee, H. Kang, H. Kim, H. A. D. Nguyen, K. Shin, *J. Mech. Sci. Technol.* **2010**, 24, 315.
- [53] C. Lee, H. Kang, C. Kim, K. Shin, *J. Microelectromech. Syst.* **2010**, 19, 1243.
- [54] H. Kang, C. Lee, *Int. J. Precis. Eng. Manuf.* **2015**, 16, 99.
- [55] N. A. Ebler, R. Arnason, G. Michaelis, N. D'Sa, *IEEE Trans. Ind. Appl.* **1993**, 29, 727.
- [56] V. Gassmann, D. Knittel, P. R. Pagilla, M.-A. Bueno, *IEEE Trans. Control Syst. Technol.* **2012**, 20, 173.
- [57] K.-H. Choi, T. T. Tran, D.-S. Kim, *J. Adv. Mech. Des. Syst. Manuf.* **2011**, 5, 7.
- [58] C. Lee, H. Kang, K. Shin, *J. Mech. Sci. Technol.* **2010**, 24, 1097.
- [59] M. Jung, Y. Kim, D. Oh, *Microsyst. Technol.* **2016**, 22, 1381.
- [60] J. Lee, J. Seong, J. Park, S. Park, D. Lee, K.-H. Shin, *Mech. Syst. Signal Process.* **2015**, 60–61, 706.

- [61] C. H. Kim, J. Jo, S.-H. Lee, *Rev. Sci. Instrum.* **2012**, *83*, 065001.
- [62] S. Garner, S. Glaesemann, X. Li, *Appl. Phys. A: Mater. Sci. Process.* **2014**, *116*, 403.
- [63] C. Deus, J. Salomon, U. Wehner, *VIP Dünnschichttechnologie* **2016**, *28*, 40.
- [64] W. A. MacDonald, M. K. Looney, D. MacKerron, R. Eveson, R. Adam, K. Hashimoto, K. Rakos, *J. SID* **2007**, *15*, 1075.
- [65] P. Schwamb, T. C. Reusch, C. J. Brabec, *Proc. SPIE* **2013**, *8829*, 88291E-1.
- [66] F.-C. Chen, J.-L. Wu, C.-L. Lee, W.-C. Huang, H.-M. P. Chen, W.-C. Chen, *IEEE Electron Dev. Lett.* **2009**, *30*, 727.
- [67] A. Chandra, M. Takashima, J. Li, P. Beck, S. Bruner, D. Tinsley, R. Sreenivasan, A. Kamath, *MRS Adv.* **2017**, *2*, 1029.
- [68] A. Hübler, B. Trnovec, T. Zillger, M. Ali, N. Wetzold, M. Mingeback, A. Wagenpfahl, C. Deibel, V. Dyakonov, *Adv. Eng. Mater.* **2011**, *1*, 1018.
- [69] S. Reineke, M. Thomschke, B. Lüssem, K. Leo, *Rev. Mod. Phys.* **2013**, *85*, 1245.
- [70] J.-W. Lee, Y.-T. Yoo, *J. Ind. Eng. Chem.* **2012**, *18*, 1647.
- [71] Z. B. Wang, M. G. Helander, X. F. Xu, D. P. Puzzo, J. Qiu, M. T. Greiner, Z. H. Lu, *J. Appl. Phys.* **2011**, *109*, 053107.
- [72] K. Sato, S. Uchida, S. Toriyama, S. Nishimura, K. Oyaizu, H. Nishide, Y. Nishikitani, *Adv. Mater. Technol.* **2017**, *2*, 1600293.
- [73] K. Ellmer, *Nat. Photonics* **2012**, *6*, 809.
- [74] C. J. M. Emmott, A. Urbina, J. Nelson, *Sol. Energy Mater. Sol. Cells* **2012**, *97*, 14.
- [75] G. Sico, M. Montanino, A. de Girolamo del Mauro, A. Imparato, G. Nobile, C. Minarini, *Org. Electron.* **2016**, *28*, 257.
- [76] M. Montanino, G. Sico, C. T. Prontera, A. de Girolamo del Mauro, S. Aprano, M. G. Maglione, C. Minarini, *EXPRESS Polym. Lett.* **2017**, *11*, 518.
- [77] J. K. Hwang, S. Bae, D. S. Kim, *Jpn. J. Appl. Phys.* **2014**, *53*, 05HC12.
- [78] G. Jo, M. Choe, S. Lee, W. Park, Y. H. Kahng, T. Lee, *Nanotechnology* **2012**, *23*, 112001.
- [79] Y. Lee, J.-H. Ahn, *Nano* **2013**, *8*, 1330001.
- [80] J. W. Jo, J. U. Lee, W. H. Jo, *Polym. Int.* **2015**, *64*, 1676.
- [81] Y. Xu, J. Liu, *Small* **2016**, *12*, 1400.
- [82] H.-W. Jang, W. S. Kim, *Appl. Phys. Lett.* **2016**, *108*, 091601.
- [83] J. Ning, L. Hao, M. Jin, X. Qiu, Y. Shen, J. Liang, X. Zhang, B. Wang, X. Li, L. Zhi, *Adv. Mater.* **2017**, *29*, 1605028.
- [84] X. Hu, L. Chen, T. Ji, Y. Zhang, A. Hu, F. Wu, G. Li, Y. Chen, *Adv. Mater. Interfaces* **2015**, *2*, 1500445.
- [85] X. Hu, X. Meng, J. Xiong, Z. Huang, X. Yang, L. Tan, Y. Chen, *Adv. Mater. Technol.* **2017**, *2*, 1700138.
- [86] X. Hu, L. Chen, Y. Zhang, Q. Hu, J. Yang, Y. Chen, *Chem. Mater.* **2014**, *26*, 6293.
- [87] L. Y. L. Wu, W. T. Kerk, C. C. Wong, *Thin Solid Films* **2013**, *544*, 427.
- [88] S. Kim, S. Y. Kim, M. H. Chung, J. Kim, J. H. Kim, *J. Mater. Chem. C* **2015**, *3*, 5859.
- [89] Q. Nian, M. Saei, Y. Xu, G. Sabyasachi, B. Deng, Y. P. Chen, G. J. Cheng, *ACS Nano* **2015**, *9*, 10018.
- [90] S. J. Lee, Y.-H. Kim, J. K. Kim, H. Baik, J. H. Park, J. Lee, J. Nam, J. H. Park, T.-W. Lee, G.-R. Yi, J. H. Cho, *Nanoscale* **2014**, *6*, 11828.
- [91] B. Deng, P.-C. Hsu, G. Chen, B. N. Chandrashekar, L. Liao, Z. Ayitumuda, J. Wu, Y. Guo, L. Lin, Y. Zhou, M. Aisijiang, Q. Xie, Y. Cui, Z. Liu, H. Peng, *Nano Lett.* **2015**, *15*, 4206.
- [92] D.-J. Kim, H.-I. Shin, E.-H. Ko, K.-H. Kim, T.-W. Kim, H.-K. Kim, *Sci. Rep.* **2016**, *6*, 34322.
- [93] R. E. Triambulo, H.-G. Cheong, J.-W. Park, *Org. Electron.* **2014**, *15*, 2685.
- [94] Z. Zhong, H. Lee, D. Kang, S. Kwon, Y.-M. Choi, I. Kim, K.-Y. Kim, Y. Lee, K. Woo, J. Moon, *ACS Nano* **2016**, *10*, 7847.
- [95] E. Jung, C. Kim, M. Kim, H. Chae, J. H. Cho, S. M. Cho, *Org. Electron.* **2017**, *41*, 190.
- [96] Q. Nian, M. Saei, Y. Hu, B. Deng, S. Jin, G. J. Cheng, *Extreme Mech. Lett.* **2016**, *9*, 531.
- [97] K. Shin, J. Park, C. Lee, *Thin Solid Films* **2016**, *598*, 95.
- [98] S. Chen, Y. Guan, Y. Li, X. Yan, H. Ni, L. Li, *J. Mater. Chem. C* **2017**, *5*, 2404.
- [99] B.-Y. Wang, E.-S. Lee, D.-S. Lim, H. W. Kang, Y.-J. Oh, *RSC Adv.* **2017**, *7*, 7540.
- [100] K. K. Sears, M. Fievez, M. Gao, H. C. Weerasinghe, C. D. Easton, D. Vak, *Sol. RRL* **2017**, *1*, 1700059.
- [101] T. Mäkelä, T. Haatainen, P. Majander, J. Ahopelto, *Microelectron. Eng.* **2007**, *84*, 877.
- [102] A. Kamysny, S. Magdassi, *Small* **2014**, *10*, 3515.
- [103] R. V. K. Rao, K. V. Abhinav, P. S. Karthik, S. P. Singh, *RSC Adv.* **2015**, *5*, 77760.
- [104] K. V. Abhinav, R. V. K. Rao, P. S. Karthik, S. P. Singh, *RSC Adv.* **2015**, *5*, 63985.
- [105] J. Woerle, H. Rost, *MRS Bull.* **2011**, *36*, 789.
- [106] H. A. D. Nguyen, K. Shin, C. Lee, *Int. J. Precis. Eng. Manuf.* **2015**, *16*, 517.
- [107] H. A. D. Nguyen, K. Shin, C. Lee, *Int. J. Adv. Manuf. Technol.* **2017**, *90*, 3595.
- [108] H. J. van de Wiel, Y. Galagan, T. J. van Lammeren, J. F. J. de Riet, J. Gilot, M. G. M. Nagelkerke, R. H. C. A. T. Lelieveld, S. Shanmugam, A. Pagudala, D. Hui, W. A. Groen, *Nanotechnology*, **2013**, *24*, 484041.
- [109] X. Zhang, K. Liu, V. Sunappan, X. Shan, *J. Mater. Process. Technol.* **2015**, *225*, 337.
- [110] D. Deganello, J. A. Cherry, D. T. Gethin, T. C. Claypole, *Thin Solid Films*, **2010**, *518*, 6113.
- [111] D. Deganello, J. A. Cherry, D. T. Gethin, T. C. Claypole, *Thin Solid Films* **2012**, *520*, 2233.
- [112] D.-Y. Shin, M. Jung, S. Chun, *J. Mater. Chem.* **2012**, *22*, 11755.
- [113] S. Chun, D. Grudin, D. Lee, S.-H. Kim, G.-R. Yi, I. Wang, *Chem. Mater.* **2009**, *21*, 343.
- [114] J. Perelaer, U. S. Schubert, *J. Mater. Res.* **2013**, *28*, 564.
- [115] S. Wüschler, R. Abbel, J. Perelaer, U. S. Schubert, *J. Mater. Chem. C* **2014**, *2*, 10232.
- [116] J. Yeo, G. Kim, S. Hong, M. S. Kim, D. Kim, J. Lee, H. B. Lee, J. Kwon, Y. D. Suh, H. W. Kang, H. J. Sung, J.-H. Choi, W.-H. Hong, J. M. Ko, S.-H. Lee, S.-H. Choa, S. H. Ko, *J. Power Sources* **2014**, *246*, 562.
- [117] E. Jansson, J. Hast, J. Petäjä, J. Honkala, J. Häkkinen, O.-H. Huttunen, *J. Print Media Technol. Res.* **2015**, *4*, 19.
- [118] J. Park, J. Lee, S. Park, K.-H. Shin, D. Lee, *Int. J. Adv. Manuf. Technol.* **2016**, *82*, 1921.
- [119] M. Pudas, N. Halonen, P. Granat, J. Vähäkangas, *Prog. Org. Coat.* **2005**, *54*, 310.
- [120] M. G. Han, J. Sperry, A. Gupta, C. F. Huebner, S. T. Ingram, S. H. Foulger, *J. Mater. Chem.* **2007**, *17*, 1347.
- [121] H. A. D. Nguyen, K.-H. Shin, D. Lee, *Jpn. J. Appl. Phys.* **2014**, *53*, 05HC04.
- [122] J. Park, H. A. D. Nguyen, S. Park, J. Lee, B. Kim, D. Lee, *Curr. Appl. Phys.* **2015**, *15*, 367.
- [123] H. A. D. Nguyen, C. Lee, K.-H. Shin, D. Lee, *IEEE Trans. Compon. Packag. Manuf. Technol.* **2015**, *5*, 1516.
- [124] E. Sowade, H. Kang, K. Y. Mitra, O. J. Weiß, J. Weber, R. R. Baumann, *J. Mater. Chem. C* **2015**, *3*, 11815.
- [125] T. M. Kraft, L. Leppänen, T. Kololuoma, S. Lahokallio, L. Frisk, M. Mäntysalo, *Proc. 6th Electron. Syst. Int. Technol. Conf.*, Grenoble, France, **2016**, 16520124.
- [126] T. Happonen, T. Ritvonen, P. Korhonen, J. Häkkinen, T. Fabritius, *Int. J. Adv. Manuf. Technol.* **2016**, *82*, 1663.
- [127] V. Sunappan, *Proc. 2016 IEEE 18th Electron. Pack. Technol. Conf.*, Singapore, **2016**, 593.

- [128] J. S. Yu, I. Kim, J.-S. Kim, J. Jo, T. T. Larsen-Olsen, R. R. Søndergaard, M. Hösel, D. Angmo, M. Jørgensen, F. C. Krebs, *Nanoscale* **2012**, 4, 6032.
- [129] K.-H. Shin, H. A. D. Nguyen, J. Park, D. Shin, D. Lee, *J. Coat. Technol. Res.* **2017**, 14, 95.
- [130] J. Noh, D. Yeom, C. Lim, H. Cha, J. Han, J. Kim, Y. Park, V. Subramanian, G. Cho, *IEEE Trans. Electron. Packag. Manuf.* **2010**, 33, 275.
- [131] K. Keränen, P. Korhonen, J. Rekilä, O. Tapaninen, T. Happonen, P. Makkonen, K. Rönkä, *Int. J. Adv. Manuf. Technol.* **2015**, 81, 529.
- [132] M. Yi, D. Yeom, W. Lee, S. Jang, G. Cho, *J. Nanosci. Nanotechnol.* **2013**, 13, 5360.
- [133] H.-C. Su, C.-Y. Cheng, *Isr. J. Chem.* **2014**, 54, 855.
- [134] Q. Sun, Y. Li, Q. Pei, *J. Disp. Technol.* **2007**, 3, 211.
- [135] A. F. Henwood, E. Zysman-Colman, *Top. Curr. Chem.* **2016**, 374, 36.
- [136] R. D. Costa (Ed.), *Light-Emitting Electrochemical Cells: Concepts, Advances and Challenges*, 1st ed., Springer International Publishing, Cham, Switzerland **2017**.
- [137] A. Asadpoorardavish, A. Sandström, C. Larsen, R. Bollström, M. Toivakka, R. Österbacka, L. Edman, *Adv. Funct. Mater.* **2015**, 25, 3238.
- [138] M. Bredol, H. Schulze Dieckhoff, *Materials* **2010**, 3, 1353.
- [139] J. W. Park, in *Organic Light-Emitting Diodes (OLEDs): Materials, Devices and Applications* (Ed: A. Buckley), Woodhead Publishing Ltd., Cambridge, United Kingdom **2013**, Ch. 19.
- [140] D. J. Gaspar, E. Polikarpov (Eds.), *OLED Fundamentals: Materials, Devices, and Processing of Organic Light-Emitting Diodes*, CRC Press, Boca Raton, United States **2015**.
- [141] A. Sandström, H. F. Dam, F. C. Krebs, L. Edman, *Nat. Commun.* **2012**, 3, 1002.
- [142] A. R. Duggal, C. M. Heller, J. J. Shiang, J. Liu, L. N. Lewis, *J. Disp. Technol.* **2007**, 3, 184.
- [143] J. Hast, M. Tuomikoski, R. Suhonen, K.-L. Väisänen, M. Välimäki, T. Maaninen, P. Apilo, A. Alastalo, A. Maaninen, *SID 2013 Digest*, Vancouver, Canada **2013**, p. 192.
- [144] S. Shin, M. Yang, L. J. Guo, H. Youn, *Small* **2013**, 9, 4036.
- [145] B. Walker, C. Kim, T.-Q. Nguyen, *Chem. Mater.* **2011**, 23, 470.
- [146] Q. Wang, Y. Xie, F. Soltani-Kordshuli, M. Eslamian, *Renewable Sustainable Energy Rev.* **2016**, 56, 347.
- [147] W. C. H. Choy, D. Zhang, *Small* **2016**, 12, 416.
- [148] M. Graetzel, R. A. J. Janssen, D. B. Mitzi, E. H. Sargent, *Nature* **2012**, 488, 304.
- [149] P. D. Matthews, D. J. Lewis, P. O'Brien, *J. Mater. Chem. A* **2017**, 5, 17135.
- [150] S. B. Darling, F. You, *RSC Adv.* **2013**, 3, 17633.
- [151] N. Espinosa, M. Hösel, D. Angmo, F. C. Krebs, *Energy Environ. Sci.* **2012**, 5, 5117.
- [152] F. C. Krebs, *Sol. Energy Mater. Sol. Cells* **2009**, 93, 465.
- [153] F. C. Krebs, *Sol. Energy Mater. Sol. Cells* **2009**, 93, 394.
- [154] R. Søndergaard, M. Hösel, D. Angmo, T. T. Larsen-Olsen, F. C. Krebs, *Mater. Today* **2012**, 15, 36.
- [155] T. M. Eggenhuisen, Y. Galagan, A. F. K. V. Biezemans, T. M. W. L. Slaats, W. P. Voorthuijzen, S. Kommeren, S. Shanmugam, J. P. Teunissen, A. Hadipour, W. J. H. Verhees, S. C. Veenstra, M. J. J. Coenen, J. Gilot, R. Andriessen, W. A. Groen, *J. Mater. Chem. A* **2015**, 3, 7255.
- [156] T. M. Eggenhuisen, Y. Galagan, E. W. C. Coenen, W. P. Voorthuijzen, M. W. L. Slaats, S. A. Kommeren, S. Shanmugan, M. J. J. Coenen, R. Andriessen, W. A. Groen, *Sol. Energy Mater. Sol. Cells* **2015**, 134, 364.
- [157] F. Machui, L. Lucera, G. D. Spyropoulos, J. Cordero, A. S. Ali, P. Kubis, T. Ameri, M. M. Voigt, C. J. Brabec, *Sol. Energy Mater. Sol. Cells* **2014**, 128, 441.
- [158] J. G. Tait, C. Wong, D. Cheyns, M. Turbiez, B. P. Rand, P. Heremans, *IEEE J. Photovolt.* **2014**, 4, 1538.
- [159] J. M. Ding, A. de la Fuente Vornbrock, C. Ting, V. Subramanian, *Sol. Energy Mater. Sol. Cells* **2009**, 93, 459.
- [160] D. Angmo, H. F. Dam, T. R. Andersen, N. K. Zawacka, M. V. Madsen, J. Stubager, F. Livi, R. Gupta, M. Helgesen, J. E. Carlé, T. T. Larsen-Olsen, G. U. Kulkarni, E. Bundgaard, F. C. Krebs, *Energy Technol.* **2014**, 2, 651.
- [161] H. F. Dam, T. R. Andersen, M. V. Madsen, T. K. Mortensen, M. F. Pedersen, U. Nielsen, F. C. Krebs, *Sol. Energy Mater. Sol. Cells* **2015**, 140, 187.
- [162] H. F. Dam, F. C. Krebs, *Sol. Energy Mater. Sol. Cells* **2012**, 97, 191.
- [163] H. W. Ro, J. M. Downing, S. Engmann, A. A. Herzing, D. M. DeLongchamp, L. J. Richter, S. Mukherjee, H. Ade, M. Abdelsamir, L. K. Jagadamma, A. Amassian, Y. Liu, H. Yan, *Energy Environ. Sci.* **2016**, 9, 2835.
- [164] K. Liu, T. T. Larsen-Olsen, Y. Lin, M. Beliatas, E. Bundgaard, M. Jørgensen, F. C. Krebs, X. Zhan, *J. Mater. Chem. A* **2016**, 4, 1044.
- [165] F. C. Krebs, *Org. Electron.* **2009**, 10, 761.
- [166] F. C. Krebs, *Sol. Energy Mater. Sol. Cells* **2009**, 93, 1636.
- [167] F. C. Krebs, S. A. Gevorgyan, J. Alstrup, *J. Mater. Chem.* **2009**, 19, 5442.
- [168] F. C. Krebs, T. Tromholt, M. Jørgensen, *Nanoscale* **2010**, 2, 873.
- [169] F. C. Krebs, J. Fyenbo, M. Jørgensen, *J. Mater. Chem.* **2010**, 20, 8994.
- [170] R. Søndergaard, M. Manceau, M. Jørgensen, F. C. Krebs, *Adv. Energy Mater.* **2012**, 2, 415.
- [171] E. Bundgaard, O. Hagemann, M. Manceau, M. Jørgensen, F. C. Krebs, *Macromolecules* **2010**, 43, 8115.
- [172] M. Helgesen, J. E. Carlé, B. Andreasen, M. Hösel, K. Norrman, R. Søndergaard, F. C. Krebs, *Polym. Chem.* **2012**, 3, 2649.
- [173] N. Espinosa, R. García-Valverde, A. Urbina, F. C. Krebs, *Sol. Energy Mater. Sol. Cells* **2011**, 95, 1293.
- [174] M. Manceau, D. Angmo, M. Jørgensen, F. C. Krebs, *Org. Electron.* **2011**, 12, 566.
- [175] D. Angmo, S. A. Gevorgyan, T. T. Larsen-Olsen, R. R. Søndergaard, M. Hösel, M. Jørgensen, R. Gupta, G. U. Kulkarni, F. C. Krebs, *Org. Electron.* **2013**, 14, 984.
- [176] D. Angmo, F. C. Krebs, *J. Appl. Polym. Sci.* **2013**, 129, 1.
- [177] D. Angmo, T. T. Larsen-Olsen, M. Jørgensen, R. R. Søndergaard, F. C. Krebs, *Adv. Energy Mater.* **2013**, 3, 172.
- [178] T. T. Larsen-Olsen, R. R. Søndergaard, K. Norrman, M. Jørgensen, F. C. Krebs, *Energy Environ. Sci.* **2012**, 5, 9467.
- [179] N. Espinosa, F. O. Lenzmann, S. Ryley, D. Angmo, M. Hösel, R. R. Søndergaard, D. Huss, S. Däfinger, S. Gritsch, J. M. Kroon, M. Jørgensen, F. C. Krebs, *J. Mater. Chem. A* **2013**, 1, 7037.
- [180] T. R. Andersen, H. F. Dam, M. Hösel, M. Helgesen, J. E. Carlé, T. T. Larsen-Olsen, S. A. Gevorgyan, J. W. Andreasen, J. Adams, N. Li, F. Machui, G. D. Spyropoulos, T. Ameri, N. Lemaître, M. Legros, A. Scheel, D. Gaiser, K. Kreul, S. Berny, O. R. Lozman, S. Nordman, M. Välimäki, M. Vilkmann, R. R. Søndergaard, M. Jørgensen, C. J. Brabec, F. C. Krebs, *Energy Environ. Sci.* **2014**, 7, 2925.
- [181] <https://infinitypv.com/>. Last accessed Dec 30, **2017**.
- [182] H.-C. Cha, Y.-C. Huang, F.-H. Hsu, C.-M. Chuang, D.-H. Lu, C.-W. Chou, C.-Y. Chen, C.-S. Tsao, *Sol. Energy Mater. Sol. Cells* **2014**, 130, 191.
- [183] Y.-C. Huang, H.-C. Cha, C.-Y. Chen, C.-S. Tsao, *Sol. Energy Mater. Sol. Cells* **2016**, 150, 10.
- [184] T. R. Andersen, N. A. Cooling, F. Almyahi, A. S. Hart, N. C. Nicolaidis, K. Feron, M. Noori, B. Vaughan, M. J. Griffith, W. J. Belcher, P. C. Dastoor, *Sol. Energy Mater. Sol. Cells* **2016**, 149, 103.
- [185] M. J. Griffith, N. A. Cooling, B. Vaughan, D. C. Elkington, A. S. Hart, A. G. Lyons, S. Quereschi, W. J. Belcher, P. C. Dastoor, *IEEE J. Sel. Top. Quantum Electron.* **2016**, 22, 4100714.

- [186] M. J. Griffith, N. A. Cooling, B. Vaughan, K. M. O'Donnell, M. F. Al-Mudhaffer, A. Al-Ahmad, M. Noori, F. Almyahi, W. J. Belcher, P. C. Dastoor, *Energy Technol.* **2015**, 3, 428.
- [187] L. M. Andersson, *Energy Technol.* **2015**, 3, 437.
- [188] Y. Galagan, E. W. C. Coenen, B. Zimmermann, L. H. Slooff, W. J. H. Verhees, S. C. Veenstra, J. M. Kroon, M. Jørgensen, F. C. Krebs, R. Andriessen, *Adv. Energy Mater.* **2014**, 4, 1300498.
- [189] Y. Galagan, B. Zimmermann, E. W. C. Coenen, M. Jørgensen, D. M. Tanenbaum, F. C. Krebs, H. Gorter, S. Sabik, L. H. Slooff, S. C. Veenstra, J. M. Kroon, R. Andriessen, *Adv. Energy Mater.* **2012**, 2, 103.
- [190] P. Kubis, L. Lucera, F. Machui, G. Spyropoulos, J. Cordero, A. Frey, J. Kaschta, M. M. Voigt, G. J. Matt, E. Zeira, C. J. Brabec, *Org. Electron.* **2014**, 15, 2256.
- [191] Y. Galagan, H. Fledderus, H. Gorter, H. H. t Mannetje, S. Shanmugam, R. Mandamparambil, J. Bosman, J.-E. J. M. Rubingh, J.-P. Teunissen, A. Salem, I. G. de Vries, R. Andriessen, W. A. Groen, *Energy Technol.* **2015**, 3, 834.
- [192] Y. Galagan, I. G. de Vries, A. P. Langen, R. Andriessen, W. J. H. Verhees, S. C. Veenstra, J. M. Kroon, *Chem. Eng. Process.* **2011**, 50, 454.
- [193] C. Kapnopoulos, E. D. Mekeridis, L. Tzounis, C. Polyzoidis, S. Tsimikli, C. Gravalidis, A. Zachariadis, A. Laskarakis, S. Logothetidis, *Mater. Today* **2016**, 3, 746.
- [194] C. Kapnopoulos, E. D. Mekeridis, L. Tzounis, C. Polyzoidis, A. Zachariadis, S. Tsimikli, C. Gravalidis, A. Laskarakis, N. Vouroutzis, S. Logothetidis, *Sol. Energy Mater. Sol. Cells* **2016**, 144, 724.
- [195] P. Apilo, J. Hiltunen, M. Välimäki, S. Heinilehto, R. Sliz, J. Hast, *Prog. Photovoltaics* **2015**, 23, 918.
- [196] P. Kopola, T. Aernouts, S. Guillerez, H. Jin, M. Tuomikoski, A. Maaninen, J. Hast, *Sol. Energy Mater. Sol. Cells* **2010**, 94, 1673.
- [197] P. Kopola, T. Aernouts, R. Sliz, S. Guillerez, M. Ylikunnari, D. Cheyns, M. Välimäki, M. Tuomikoski, J. Hast, G. Jabbour, R. Myllylä, A. Maaninen, *Sol. Energy Mater. Sol. Cells* **2011**, 95, 1344.
- [198] M. Välimäki, P. Apilo, R. Po, E. Jansson, A. Bernardi, M. Ylikunnari, M. Vilkman, G. Corso, J. Puustinen, J. Tuominen, J. Hast, *Nanoscale* **2015**, 7, 9570.
- [199] M. Välimäki, E. Jansson, P. Korhonen, A. Peltoniemi, S. Rousu, *Nanoscale Res. Lett.* **2017**, 12, 117.
- [200] M. Vilkman, P. Apilo, M. Välimäki, M. Ylikunnari, A. Bernardi, R. Po, G. Corso, J. Hast, *Energy Technol.* **2015**, 3, 407.
- [201] M. M. Voigt, R. C. I. Mackenzie, S. P. King, C. P. Yau, P. Atienzar, J. Dane, P. E. Keivanidis, I. Zadrazil, D. D. C. Bradley, J. Nelson, *Sol. Energy Mater. Sol. Cells* **2012**, 105, 77.
- [202] M. M. Voigt, R. C. I. Mackenzie, C. P. Yau, P. Atienzar, J. Dane, P. E. Keivanidis, D. D. C. Bradley, J. Nelson, *Sol. Energy Mater. Sol. Cells* **2011**, 95, 731.
- [203] D. Vak, H. Weerasinghe, J. Ramamurthy, J. Subbiah, M. Brown, D. J. Jones, *Sol. Energy Mater. Sol. Cells* **2016**, 149, 154.
- [204] Y. Galagan, H. Fledderus, H. Gorter, H. H. t Mannetje, S. Shanmugam, R. Mandamparambil, J. Bosman, J.-E. J. M. Rubingh, J.-P. Teunissen, A. Salem, I. G. de Vries, R. Andriessen, W. A. Groen, *Energy Technol.* **2015**, 3, 791.
- [205] <https://www.eight19.com/>. Last accessed Dec 30, **2017**.
- [206] <http://www.opvius.com/>. Last accessed Dec 30, **2017**.
- [207] <http://www.armor-group.com/en>. Last accessed Dec 30, **2017**.
- [208] [http://www.asca.com/index\\_en.html](http://www.asca.com/index_en.html). Last accessed Dec 30, **2017**.
- [209] <http://www.csembrasil.com.br/p/>. Last accessed Dec 30, **2017**.
- [210] <http://www.sunew.com.br/>. Last accessed Dec 30, **2017**.
- [211] F. C. Krebs, J. Fyenbo, D. M. Tanenbaum, S. A. Gevorgyan, R. Andriessen, B. van Remoortere, Y. Galagan, M. Jørgensen, *Energy Environ. Sci.* **2011**, 4, 4116.
- [212] N. Espinosa, M. Hösel, M. Jørgensen, F. C. Krebs, *Energy Environ. Sci.* **2014**, 7, 855.
- [213] F. C. Krebs, N. Espinosa, M. Hösel, R. R. Søndergaard, M. Jørgensen, *Adv. Mater.* **2014**, 26, 29.
- [214] I. Burgués-Ceballos, M. Stella, P. Lacharmoise, E. Martínez-Ferrero, *J. Mater. Chem. A* **2014**, 2, 17711.
- [215] R. Po, A. Bernardi, A. Calabrese, C. Carbonera, G. Corso, A. Pellegrino, *Energy Environ. Sci.* **2014**, 7, 925.
- [216] D. Kaduwal, H.-F. Schleiermacher, J. Schulz-Gericke, T. Kroyer, B. Zimmermann, U. Würfel, *Sol. Energy Mater. Sol. Cells* **2014**, 124, 92.
- [217] B. P. Lyons, N. Clarke, C. Groves, *Energy Environ. Sci.* **2012**, 5, 7657.
- [218] B. Ray, M. A. Alam, *Sol. Energy Mater. Sol. Cells* **2012**, 99, 204.
- [219] S. Nam, J. Jang, H. Cha, J. Hwang, T. K. An, S. Park, C. E. Park, *J. Mater. Chem.* **2012**, 22, 5543.
- [220] C. Schaefer, P. van der Schoot, J. J. Michels, *Phys. Rev. E* **2015**, 91, 022602.
- [221] C. Koidis, S. Logothetidis, S. Kassavetis, C. Kapnopoulos, P. G. Karagiannidis, D. Georgiou, A. Laskarakis, *Sol. Energy Mater. Sol. Cells* **2013**, 112, 36.
- [222] P. Westacott, N. D. Treat, J. Martin, J. H. Bannock, J. C. de Mello, M. Chabiny, A. B. Sieval, J. J. Michels, N. Stingelin, *J. Mater. Chem. A* **2017**, 5, 2689.
- [223] J. J. Michels, E. Moons, *Macromolecules* **2013**, 46, 8693.
- [224] F. C. Krebs, M. Jørgensen, *Adv. Opt. Mater.* **2014**, 2, 465.
- [225] [http://www.nrel.gov/ncpv/images/efficiency\\_chart.jpg](http://www.nrel.gov/ncpv/images/efficiency_chart.jpg). Last accessed Dec 30, **2017**.
- [226] S. A. Gevorgyan, M. V. Madsen, H. F. Dam, M. Jørgensen, C. J. Fell, K. F. Anderson, B. C. Duck, A. Mescheloff, E. A. Katz, A. Elschner, R. Roesch, H. Hoppe, M. Hermenau, M. Riede, F. C. Krebs, *Sol. Energy Mater. Sol. Cells* **2013**, 116, 187.
- [227] J. U. Lee, J. W. Jung, J. W. Jo, W. H. Jo, *J. Mater. Chem.* **2012**, 22, 24265.
- [228] A. Polman, M. Knight, E. C. Garnett, B. Ehrler, W. C. Sinke, *Science* **2016**, 352, 307.
- [229] J.-P. Correa-Baena, A. Abate, M. Saliba, W. Tress, T. J. Jacobsson, M. Grätzel, A. Hagfeldt, *Energy Environ. Sci.* **2017**, 10, 710.
- [230] M. L. Petrus, J. Schlipf, C. Li, T. P. Gujar, N. Giesbrecht, P. Müller-Buschbaum, M. Thelakkt, T. Bein, S. Hüttner, P. Docampo, *Adv. Energy Mater.* **2017**, 7, 1700264.
- [231] Y. Zhou, K. Zhu, *ACS Energy Lett.* **2016**, 1, 64.
- [232] N.-G. Park, M. Grätzel, T. Miyasaka (Eds.), *Organic-Inorganic Halide Perovskite Photovoltaics - From Fundamentals to Device Architectures*, Springer International Publishing, Cham, Switzerland **2016**.
- [233] I. Celik, Z. Song, A. J. Cimaroli, Y. Yan, M. J. Heben, D. Apul, *Sol. Energy Mater. Sol. Cells* **2016**, 156, 157.
- [234] N. Espinosa, L. Serrano-Luján, A. Urbina, F. C. Krebs, *Sol. Energy Mater. Sol. Cells* **2015**, 137, 303.
- [235] <https://www.nrel.gov/pv/assets/images/efficiency-chart.png>. Last accessed Dec 30, **2017**.
- [236] M. Yang, Y. Zhou, Y. Zeng, C.-S. Jiang, N. P. Padture, K. Zhu, *Adv. Mater.* **2015**, 27, 6363.
- [237] Y. Galagan, E. W. C. Coenen, W. J. H. Verhees, R. Andriessen, *J. Mater. Chem. A* **2016**, 4, 5700.
- [238] G. Mincuzzi, A. L. Palma, A. di Carlo, T. M. Brown, *ChemElectroChem* **2016**, 3, 9.
- [239] F. Matteocci, S. Razza, F. di Giacomo, S. Casaluci, G. Mincuzzi, T. M. Brown, A. D'Epifanio, S. Licoccia, A. di Carlo, *Phys. Chem. Chem. Phys.* **2014**, 16, 3918.
- [240] S. Razza, F. di Giacomo, F. Matteocci, L. Cinà, A. L. Palma, S. Casaluci, P. Cameron, A. D'Epifanio, S. Licoccia, A. Reale, T. M. Brown, A. di Carlo, *J. Power Sources* **2015**, 277, 286.
- [241] J. Seo, S. Park, Y. C. Kim, N. J. Jeon, J. H. Noh, S. C. Yoon, S. I. Seok, *Energy Environ. Sci.* **2014**, 7, 2642.

- [242] G. Sfyri, C. V. Kumar, D. Raptis, V. Dracopoulos, P. Lianos, *Sol. Energy Mater. Sol. Cells* **2015**, 134, 60.
- [243] F. Matteocci, L. Cinà, F. di Giacomo, S. Razza, A. L. Palma, A. Guidobaldi, A. D'Epifanio, S. Licoccia, T. M. Brown, A. Reale, A. di Carlo, *Prog. Photovoltaics* **2016**, 24, 436.
- [244] K. Cao, Z. Zuo, J. Cui, Y. Shen, T. Moehl, S. M. Zakeeruddin, M. Grätzel, M. Wang, *Nano Energy* **2015**, 17, 171.
- [245] a) Z. Wei, H. Chen, K. Yan, S. Yang, *Angew. Chem.* **2014**, 126, 13455; b) Z. Wei, H. Chen, K. Yan, S. Yang, *Angew. Chem. Int. Ed.* **2014**, 53, 13239.
- [246] Y. Deng, E. Peng, Y. Shao, Z. Xiao, Q. Dong, J. Huang, *Energy Environ. Sci.* **2015**, 8, 1544.
- [247] Y. Deng, Q. Wang, Y. Yuan, J. Huang, *Mater. Horiz.* **2015**, 2, 578.
- [248] Q. Hu, H. Wu, J. Sun, D. Yan, Y. Gao, J. Yang, *Nanoscale* **2016**, 8, 5350.
- [249] Z. Yang, C.-C. Chueh, F. Zuo, J. H. Kim, P.-W. Liang, A. K. Y. Jen, *Adv. Energy Mater.* **2015**, 5, 1500328.
- [250] S. Das, B. Yang, G. Gu, P. C. Joshi, I. N. Ivanov, C. M. Rouleau, T. Aytug, D. B. Geohegan, K. Xiao, *ACS Photonics* **2015**, 2, 680.
- [251] A. Priyadarshi, L. J. Haur, P. Murray, D. Fu, S. Kulkarni, G. Xing, T. C. Sum, N. Mathews, S. G. Mhaisalkar, *Energy Environ. Sci.* **2016**, 9, 3687.
- [252] Y. Hu, S. Si, A. Mei, Y. Rong, H. Liu, X. Li, H. Han, *Solar RRL* **2017**, 1, 1600019.
- [253] L. Cai, L. Liang, J. Wu, B. Ding, L. Gao, B. Fan, *J. Semicond.* **2017**, 38, 014006.
- [254] T. M. Schmidt, T. T. Larsen-Olsen, J. E. Carlé, D. Angmo, F. C. Krebs, *Adv. Energy Mater.* **2015**, 5, 1500569.
- [255] K. Hwang, Y.-S. Jung, Y.-J. Heo, F. H. Scholes, S. E. Watkins, J. Subbiah, D. J. Jones, D.-Y. Kim, D. Vak, *Adv. Mater.* **2015**, 27, 1241.
- [256] <http://solliance.eu/nl/solliance-realizes-a-first-up-scaled-perovskite-based-pv-module-with-10-efficiency/>. Last accessed Dec 30, **2017**.
- [257] <http://solliance.eu/nl/solliance-sets-world-record-for-roll-to-roll-produced-perovskite-based-solar-cells-with-a-stabilized-efficiency-of-126/>. Last accessed Dec 30, **2017**.
- [258] F. di Giacomo, S. Shanmugam, H. Fledderus, B. J. Bruijners, W. J. H. Verhees, M. S. Dorenkamper, S. C. Veenstra, W. Qiu, R. Gehlhaar, T. Merckx, T. Aernouts, R. Andriessen, Y. Galagan, *Sol. Energy Mater. Sol. Cells* **2017**. In press. <https://dx.doi.org/10.1016/j.solmat.2017.11.010>.
- [259] <https://solliance.eu/solliance-sets-14-5-cell-performance-record-on-large-perovskite-modules/>. Last accessed Apr 23, **2017**.
- [260] <https://solliance.eu/solliance-sets-more-world-records-for-r2r-perovskite-solar-cells-and-modules/>. Last accessed Dec 30, **2017**.
- [261] H. Sirringhaus, *Adv. Mater.* **2005**, 17, 2411.
- [262] D. Natali, M. Caironi, *Adv. Mater.* **2012**, 24, 1357.
- [263] M. Jung, J. Kim, J. Noh, N. Lim, C. Lim, G. Lee, J. Kim, H. Kang, K. Jung, A. D. Leonard, J. M. Tour, G. Cho, *IEEE Trans. Electron. Dev.* **2010**, 57, 571.
- [264] G. Klink, E. Hammerl, A. Drost, D. Hemmetzberger, K. Bock, *Proc. Polytron. 2005*, IEEE (Institute of Electrical and Electronics Engineers), Wroclaw, Poland **2005**, 1.
- [265] R. Bollström, D. Tobjörk, P. Dolietis, P. Salminen, J. Preston, R. Österbacka, M. Toivakka, *Chem. Eng. Process.* **2013**, 68, 13.
- [266] J. Noh, M. Jung, K. Jung, G. Lee, J. Kim, S. Lim, D. Kim, Y. Choi, Y. Kim, V. Subramanian, G. Cho, *IEEE Electron. Devi. Lett.* **2011**, 32, 638.
- [267] H. Park, H. Kang, Y. Lee, Y. Park, J. Noh, G. Cho, *Nanotechnology* **2012**, 23, 344006.
- [268] H. Koo, W. Lee, Y. Choi, J. Sun, J. Bak, J. Noh, V. Subramanian, Y. Azuma, Y. Majima, G. Cho, *Sci. Rep.* **2015**, 5, 14459.
- [269] C. Kim, S. W. Jeon, C. H. Kim, *Meas. Sci. Technol.* **2017**, 28, 125002.
- [270] J. Kim, T. Hassinen, W. H. Lee, S. Ko, *Org. Electron.* **2017**, 42, 361.
- [271] J. Noh, M. Jung, Y. Jung, C. Yeom, M. Pyo, G. Cho, *Proc. IEEE* **2015**, 103, 554.
- [272] M. Vilkman, T. Ruotsalainen, K. Solehmainen, E. Jansson, J. Hiitola-Keinänen, *Electronics* **2016**, 5, 2.
- [273] M. Hambach, K. Reuter, M. Stanel, G. Schmidt, H. Kempa, U. Fügmann, U. Hahn, A. C. Hübler, *Mater. Sci. Eng. B* **2010**, 170, 93.
- [274] J. Noh, M. Jung, K. Jung, G. Lee, S. Lim, D. Kim, S. Kim, James M. Tour, G. Cho, *Org. Electron.* **2011**, 12, 2185.
- [275] J. Chen, C. T. Liu, *IEEE Access* **2013**, 1, 150.
- [276] H. Kang, H. Park, Y. Park, M. Jung, B. C. Kim, G. Wallace, G. Cho, *Sci. Rep.* **2014**, 4, 5387.
- [277] M. Vilkman, T. Hassinen, M. Keränen, R. Pretot, P. van der Schaaf, T. Ruotsalainen, H. G. O. Sandberg, *Org. Electron.* **2015**, 20, 8.
- [278] Y. Jung, H. Park, J.-A. Park, J. Noh, Y. Choi, M. Jung, K. Jung, M. Pyo, K. Chen, A. Javey, G. Cho, *Sci. Rep.* **2015**, 5, 8105.
- [279] W. Lee, H. Koo, J. Sun, J. Noh, K.-S. Kwon, C. Yeom, Y. Choi, K. Chen, A. Javey, G. Cho, *Sci. Rep.* **2015**, 5, 17707.
- [280] C. M. Homenick, R. James, G. P. Lopinski, J. Dunford, J. Sun, H. Park, Y. Jung, G. Cho, P. R. L. Malenfant, *ACS Appl. Mater. Interfaces* **2016**, 8, 27900.
- [281] F. Pastorelli, T. M. Schmidt, M. Hösel, R. R. Søndergaard, M. Jørgensen, F. C. Krebs, *Adv. Eng. Mater.* **2016**, 18, 51.
- [282] Y. Zhiquan, N. Ruisheng, S. Bin, *Procedia CIRP* **2015**, 845.
- [283] S. Schaefer, D. Zipperer, *Proc. Dig. Fabr. Conf., International Conference on Digital Printing Technologies*, Seattle, United States, **2013**, 366.
- [284] R. A. Potyrailo, A. Burns, C. Surman, D. J. Lee, E. McGinniss, *Analyst* **2012**, 137, 2777.
- [285] H. Lee, D. Lee, J. Hwang, D. Nam, C. Byeon, S. H. Ko, S. Lee, *Opt. Express* **2014**, 22, 8919.
- [286] J. J. Saarinen, T. Remonen, D. Tobjörk, H. Aarnio, R. Bollström, R. Österbacka, M. Toivakka, *Packag. Technol. Sci.* **2017**, 30, 219.
- [287] C. M. Fung, J. S. Lloyd, S. Samavat, D. Deganello, K. S. Teng, *Sens. Actuators B Chem.* **2017**, 247, 807.
- [288] M. Sajid, H. W. Dang, K.-H. Na, K. H. Choi, *Sens. Actuators A* **2015**, 236, 73.
- [289] M. Cakmak, S. Batra, B. Yalcin, *Polym. Eng. Sci.* **2015**, 55, 34.
- [290] S. Batra, E. Unsal, M. Cakmak, *Adv. Funct. Mater.* **2014**, 24, 7698.
- [291] Y. Guo, S. Batra, Y. Chen, E. Wang, M. Cakmak, *ACS Appl. Mater. Interfaces* **2016**, 8, 18471.
- [292] Y. Chen, Y. Guo, S. Batra, E. Unsal, E. Wang, Y. Wan, X. Liu, Y. Wang, M. Cakmak, *RSC Adv.* **2015**, 5, 92071.
- [293] Y. Guo, Y. Chen, E. Wang, M. Cakmak, *ACS Appl. Mater. Interfaces* **2017**, 9, 919.
- [294] T. Yamashita, S. Takamatsu, K. Miyake, T. Itoh, *IEICE Electron. Express* **2012**, 9, 1442.
- [295] R. R. Søndergaard, M. Hösel, M. Jørgensen, F. C. Krebs, *J. Polym. Sci. Part B: Polym. Phys.* **2013**, 51, 132.
- [296] C.-Y. Lo, J. Hiitola-Keinänen, O.-H. Huttunen, J. Petäjä, J. Hast, A. Maaninen, H. Kopola, H. Fujita, H. Toshiyoshi, *Microelectron. Eng.* **2009**, 86, 979.
- [297] C.-Y. Lo, O.-H. Huttunen, J. Hiitola-Keinänen, J. Petäjä, H. Fujita, H. Toshiyoshi, *J. Microelectromech. Syst.* **2010**, 19, 410.